Multi-Task Bayesian Compressive Sensing for microwave imaging exploiting multi-frequency data

L. Poli, G. Oliveri, A. Massa

Abstract

This report deals with the multi-frequency Multi-Task Bayesian Compressive Sensing (BCS) technique for retrieving the dielectric features of sparse scatterers within an inaccessible investigation domain. A calibration of the MT-BCS method is firstly proposed, before to evaluate the performance of the algorithm on a wide set of scatterer configurations, showing that additional information can be educed from different illumination frequencies to improve the quality of the reconstructions. The impact of the number of frequencies exploited during the reconstruction process on the results is also investigated.

Contents

1 Calibration

1.1 Square Cylinder $l = 0.33\lambda$

Goal: show the performances of BCS when dealing with a sparse scatterer

- Number of frequencies F
- Number of Views: V
- Number of Measurements: M
- Number of Cells for the Inversion: N
- Number of Cells for the Direct solver: D
- Side of the investigation domain: L

Test Case Description

Direct solver:

- Square domain divided in $\sqrt{D} \times \sqrt{D}$ cells
- Domain side: $L = 3\lambda$
- $D = 1296$ (discretization for the direct solver: $< \lambda/10$)

Investigation domain:

- Square domain divided in $\sqrt{N} \times \sqrt{N}$ cells
- $L = 3\lambda$
- $2ka = 2 \times \frac{2\pi}{\lambda} \times \frac{L\sqrt{2}}{2} = 6\pi\sqrt{2} = 26.65$
- $\#DOF = \frac{(2ka)^2}{2} = \frac{(2\times\frac{2\pi}{\lambda}\times\frac{L\sqrt{2}}{2})^2}{2} = 4\pi^2\left(\frac{L}{\lambda}\right)^2 = 4\pi^2 \times 9 \approx 355.3$
- N scelto in modo da essere vicino a $\#DOF$: $N = 324$ (18×18)

Measurement domain:

- Measurement points taken on a circle of radius $\rho = 3\lambda$
- $M \approx 2ka \rightarrow M = 27$

Sources:

- $V = 1$ $(\theta = 0°)$
- Amplitude: $A = 1$ (plane waves)
- Number of Frequencies: $F =\in \{3, 5, 7, 9, 11, 13\}$ (selected around a central frequency $F_c = 300$ MHz)
- Frequency Range: $I_F = \{100, 120, 140, 160, 180, 200, 220\,240, 260, 280, 300, 320, 340, 360, 380, 400\}$Mhz

Object:

- Square cylinder of side $\frac{\lambda}{3} = 0.3333$
- $\varepsilon_r = 2.0$
- $\sigma = 0$ [S/m]

BCS parameters:

- Gamma prior on noise variance parameter: $\beta_1 \in \left\{1\times10^{-1},\, 2\times10^{-1},\, 5\times10^{-1},\, 1\times10^{0},\, 2\times10^{0},\, 5\times10^{0},\, 1\times10^{+1},\, 2\times10^{+1},\, 5\times10^{+1}, 1\times 1 1\times10^{+2}\right\}$
- Gamma prior on noise variance parameter: $\beta_2 \in \left\{1\times10^{+0},\, 5\times10^{-1},\, 2\times10^{-1}\,, 1\times10^{-1},\, 5\times10^{-2},\, 2\times10^{-2}\, 1\times10^{-2},, 5\times10^{-3},\, 2\times10^{-3},\, 1\times10^{-3}\right\}$
- Convergenze parameter: $\tau = 1.0\times10^{-8}$

β_1 **and** β_2 **Calibration - Noiseless**

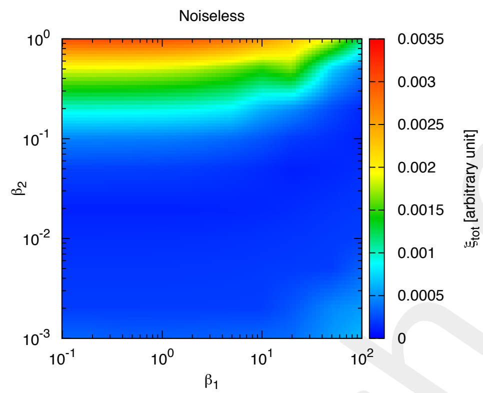

(a)

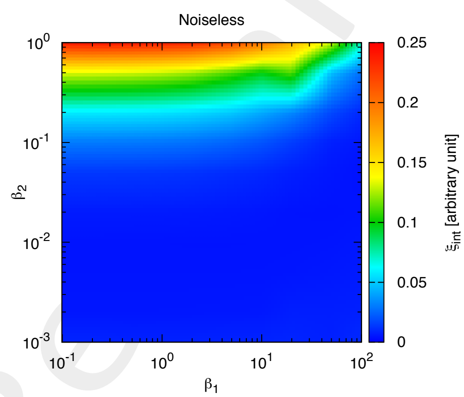

(b)

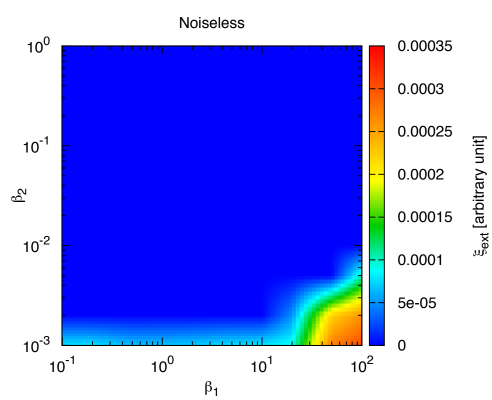

(c)

Figure 1. Noiseless - Total error ξ_{tot} (a), internal error ξ_{int} (b) and external error ξ_{ext} (c).

β_1 and β_2 Calibration - $SNR = 20$ [dB]

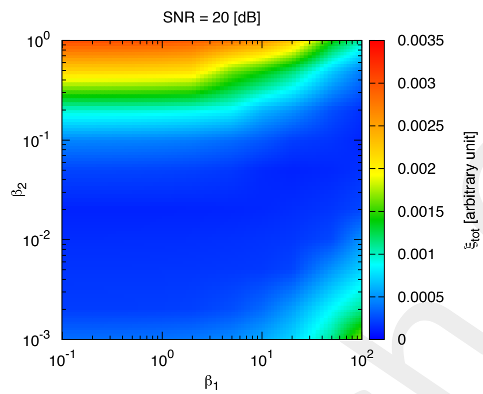

(a)

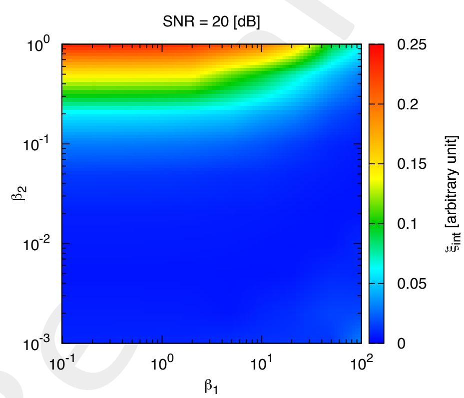

(b)

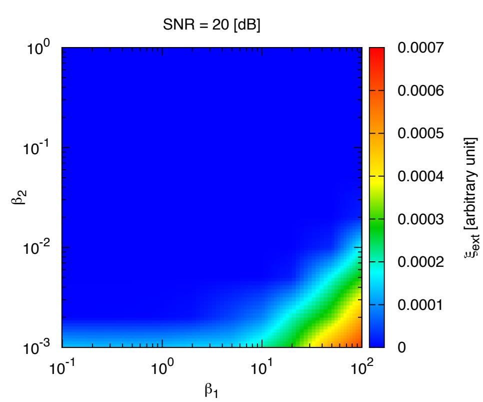

(c)

Figure 2. $SNR = 20$ [dB] - Total error ξ_{tot} (a), internal error ξ_{int} (b) and external error ξ_{ext} (c).

β_1 and β_2 Calibration - $SNR = 10$ [dB]

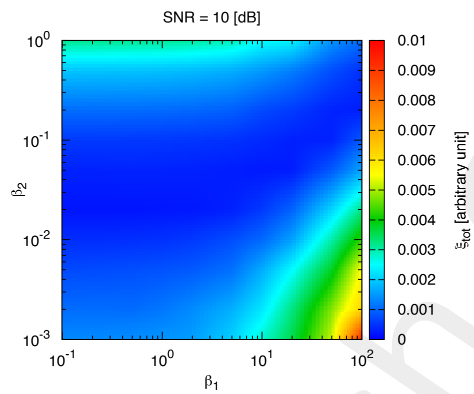

(a)

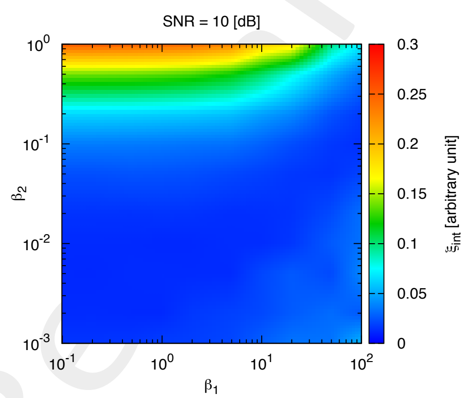

(b)

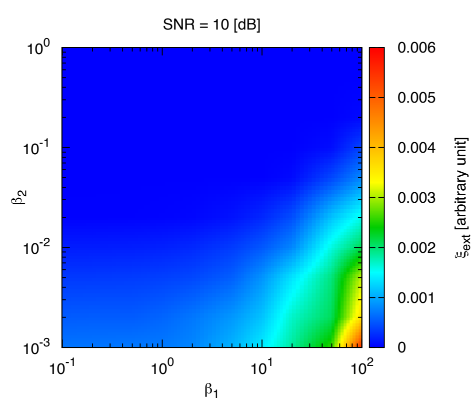

(c)

Figure 3. $SNR = 10$ [dB] - Total error ξ_{tot} (a), internal error ξ_{int} (b) and external error ξ_{ext} (c).

β_1 and β_2 Calibration - $SNR = 5$ [dB]

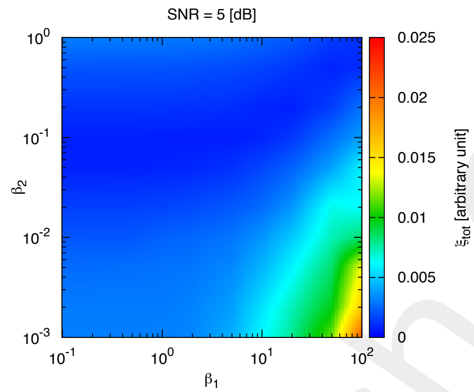

(a)

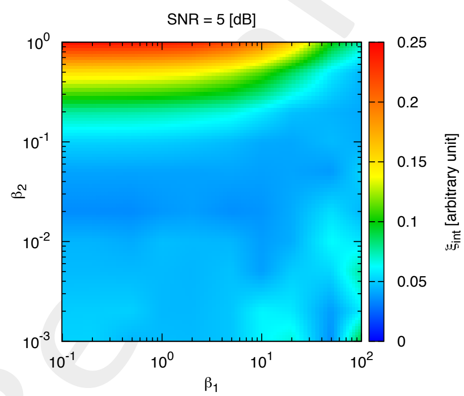

(b)

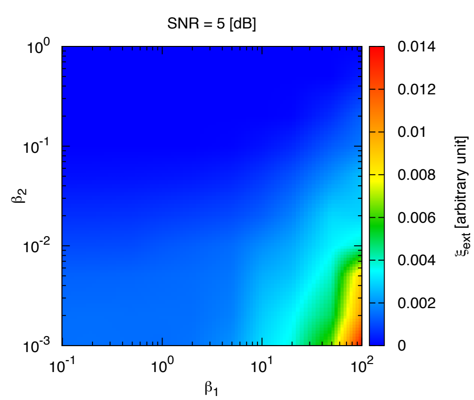

(c)

Figure 4. $SNR = 5$ [dB] - Total error ξ_{tot} (a), internal error ξ_{int} (b) and external error ξ_{ext} (c).

β_1 **and** β_2 **Calibration - Average**

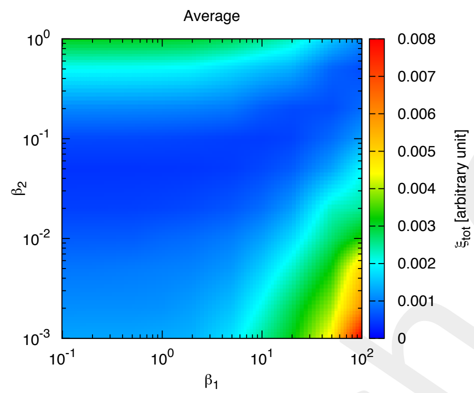

(a)

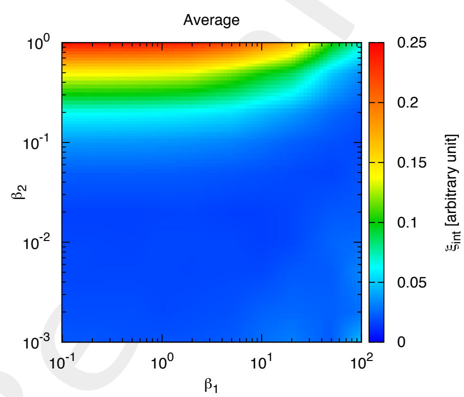

(b)

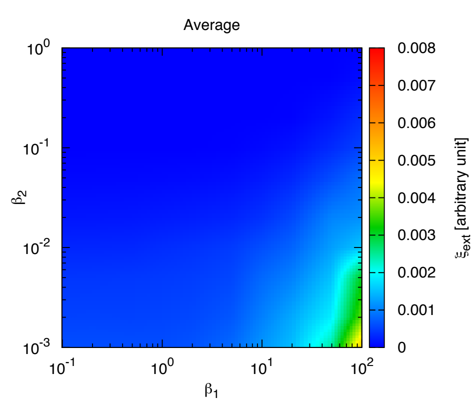

(c)

Figure 5. Average - Total error ξ_{tot} (a), internal error ξ_{int} (b) and external error ξ_{ext} (c).

Obervations:

The error function ξ_{tot} (averaged considering different SNR values: Noiseless, $SNR = 20dB$, $SNR = 10dB$ and $SNR = 5dB$) depending on the parameters (β_1, β_2) has a global minimum in ($a = 6.5 \times 10^{-1}$, $b = 5.8 \times 10^{-2}$).

Nr. Frequencies (F) Calibration

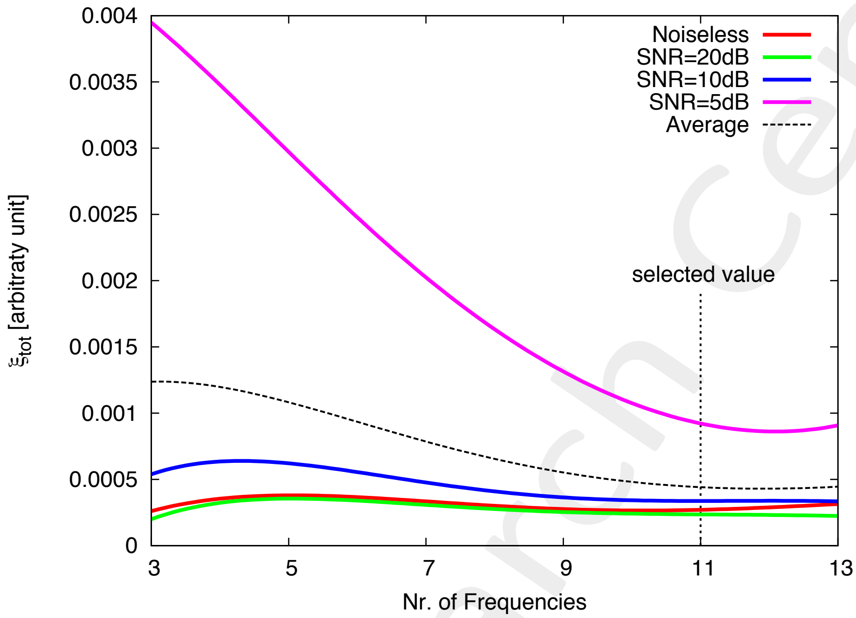

Figure 6. Total error ξ_{tot} vs. Nr. of Frequencies F.

Frequency Range (I_F) Calibration

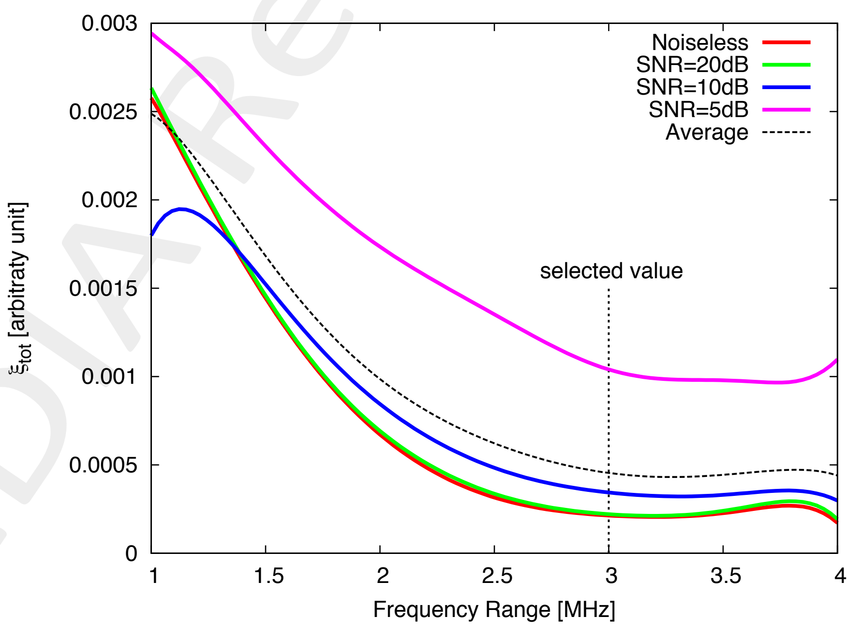

Figure 7. Total error ξ_{tot} vs. Frequency Range I_F.

2 Basic Tests

2.1 Homogeneous Objects

2.1.1 Strip of Sides $l_1 = 0.16\lambda$, $l_2 = 0.50\lambda$

Goal: show the performances of the multi-frequency $MT-BCS$ when dealing with a sparse scatterer

- Number of frequencies F
- Number of Views: V
- Number of Measurements: M
- Number of Cells for the Inversion: N
- Number of Cells for the Direct solver: D
- Side of the investigation domain: L

Test Case Description

Direct solver:

- Square domain divided in $\sqrt{D} \times \sqrt{D}$ cells
- Domain side: $L = 3\lambda$ (at the central frequency)
- $D = 1296$ (discretization for the direct solver: $< \lambda/10$)

Investigation domain:

- Square domain divided in $\sqrt{N} \times \sqrt{N}$ cells
- $L = 3\lambda$
- $2ka = 2 \times \frac{2\pi}{\lambda} \times \frac{L\sqrt{2}}{2} = 6\pi\sqrt{2} = 26.65$
- $\#DOF = \frac{(2ka)^2}{2} = \frac{(2\times\frac{2\pi}{\lambda}\times\frac{L\sqrt{2}}{2})^2}{2} = 4\pi^2\left(\frac{L}{\lambda}\right)^2 = 4\pi^2 \times 9 \approx 355.3$
- N scelto in modo da essere vicino a $\#DOF$: $N = 324$ (18×18)

Measurement domain:

- Measurement points taken on a circle of radius $\rho = 3\lambda$ (at the central frequency)
- $M \approx 2ka \rightarrow M = 27$

Sources:

- $V = 1$ $(\theta = 0°)$
- Amplitude: $A = 1$ (plane waves)
- Number of Frequencies: $F = 11$
- Frequency Range: $I_F = [150\,Mhz\,:\,450MHz]$ - Frequency Step: $S_F = [30\,Mhz]$

Object:

- Strip of sides $l_1 = 0.16\lambda$, $l_2 = 0.50\lambda$
- $\varepsilon_r = \in \{1.5, 2.0, 2.5, 3.0, 3.5, 4.0, 4.5, 5.0\}$
- $\sigma = 0$ [S/m]

MT-BCS parameters:

- Gamma prior on noise variance parameters: $\beta_1 = 6.5 \times 10^{-1}$, $\beta_2 = 5.8 \times 10^{-2}$
- Convergenze parameter: $\tau = 1.0 \times 10^{-8}$

Homogeneous Strip of Sides $l_1 = 0.16\lambda$, $l_2 = 0.50\lambda$ - Reconstruction Profiles

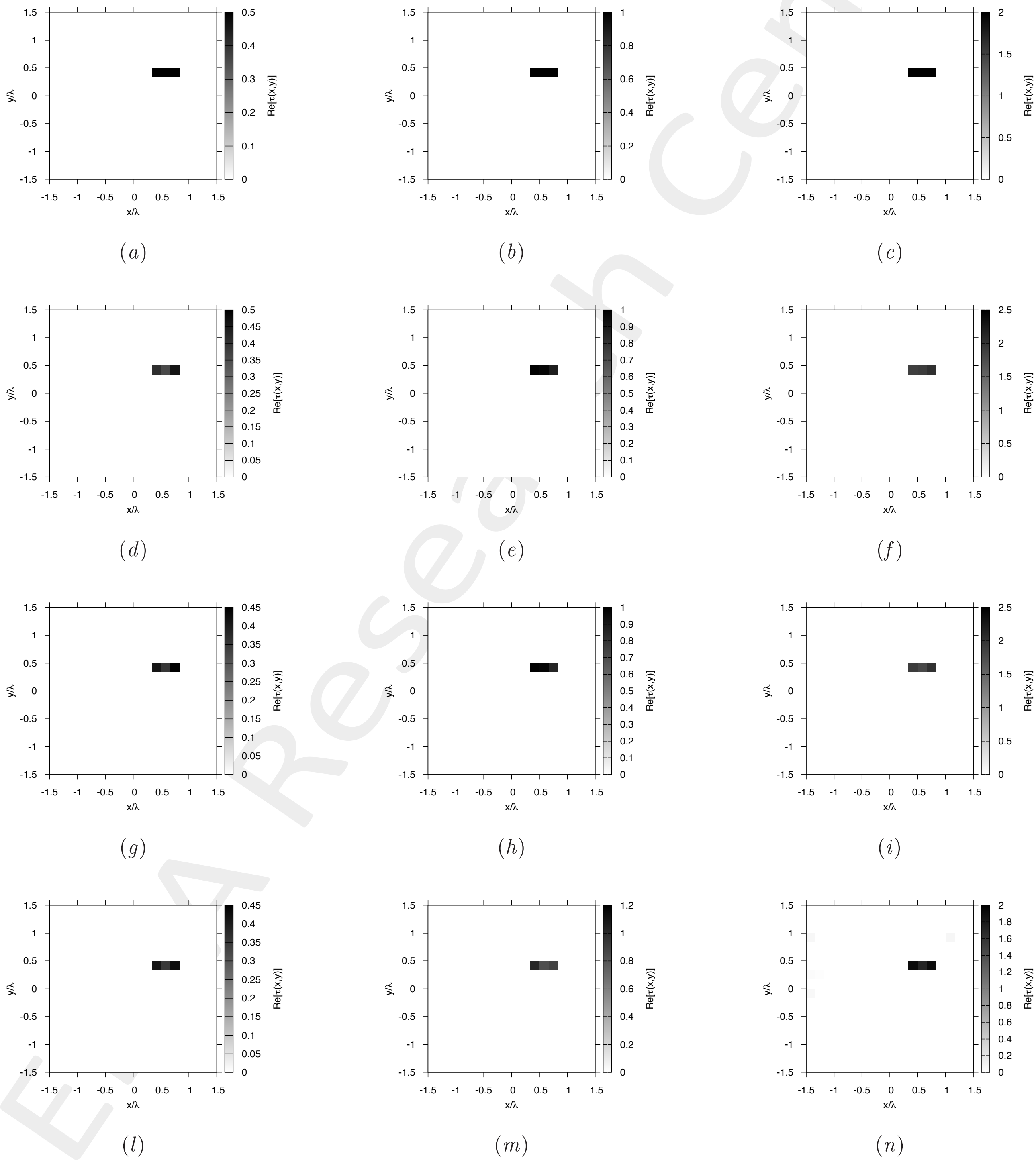

Figure 8. Actual object $(a)(b)(c)$ and MF-MT-BCS reconstructed object with $\varepsilon_r = 1.5$ $(d)(g)(l)$, $\varepsilon_r = 2.0$ $(e)(h)(m)$, and $\varepsilon_r = 3.0$ $(f)(i)(n)$, for $SNR = 20$ [dB] $(d)(e)(f)$, $SNR = 10$ [dB] $(g)(h)(i)$ and $SNR = 5$ [dB] $(l)(m)(n)$.

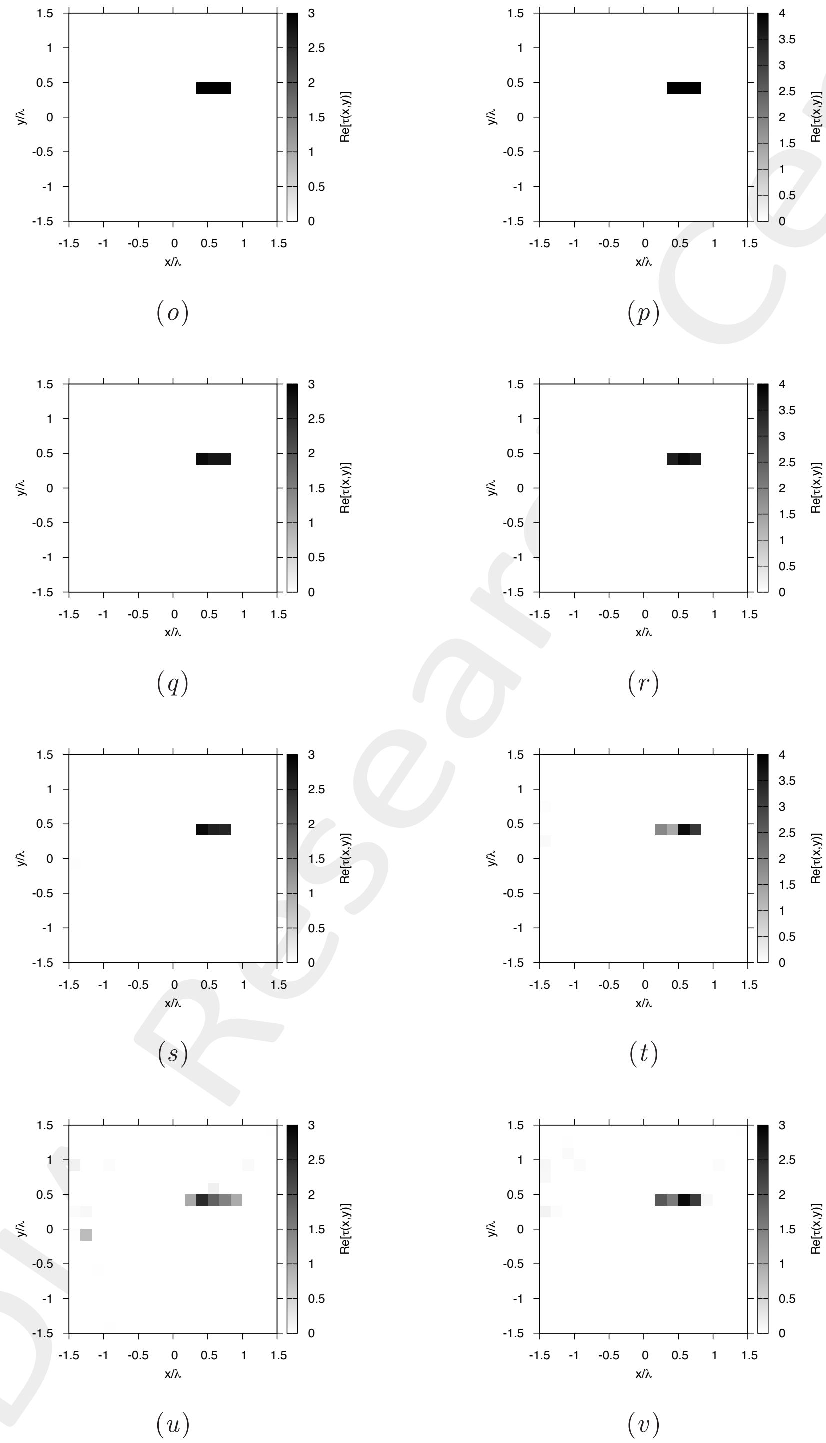

Figure 8. Actual object $(o)(p)$ and MF-MT-BCS reconstructed object with $\varepsilon_r = 4.0$ $(q)(s)(u)$, $\varepsilon_r = 5.0$ $(r)(t)(v)$, for $SNR = 20$ [dB] $(q)(r)$, $SNR = 10$ [dB] $(s)(t)$ and $SNR = 5$ [dB] $(u)(v)$.

Homogeneous Strip of Sides $l_1 = 0.16\lambda$, $l_2 = 0.50\lambda$ - Error Figures vs. ε_r

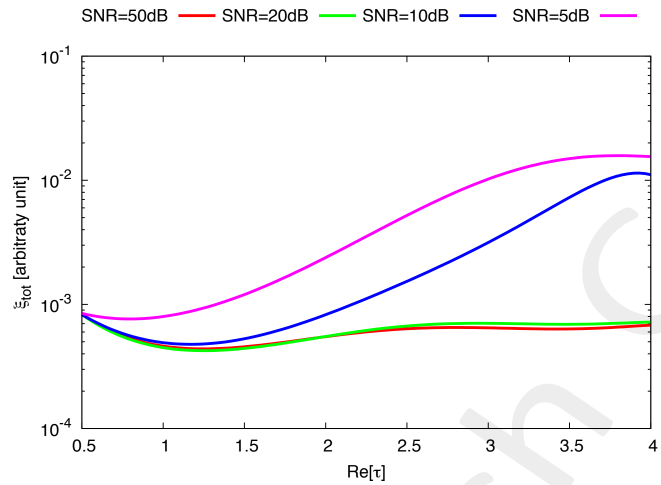

(a)

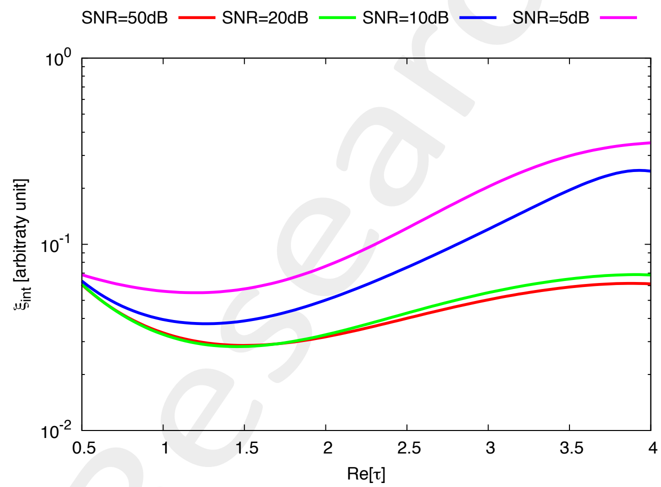

(b)

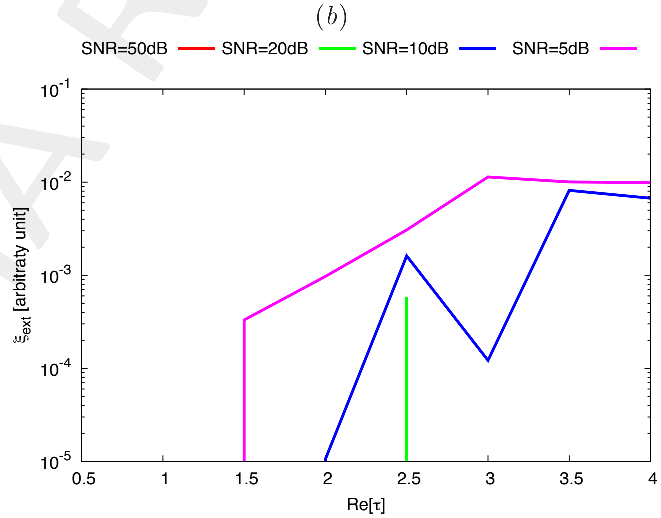

(c)

Figure 9. Behaviour of error figures as a function of ε_r, for different SNR values: (a) total error ξ_{tot}, (b) internal error ξ_{int}, (c) external error ξ_{ext}.

Homogeneous Strip of Sides $l_1 = 0.16\lambda$, $l_2 = 0.50\lambda$ - Error Figures vs. SNR

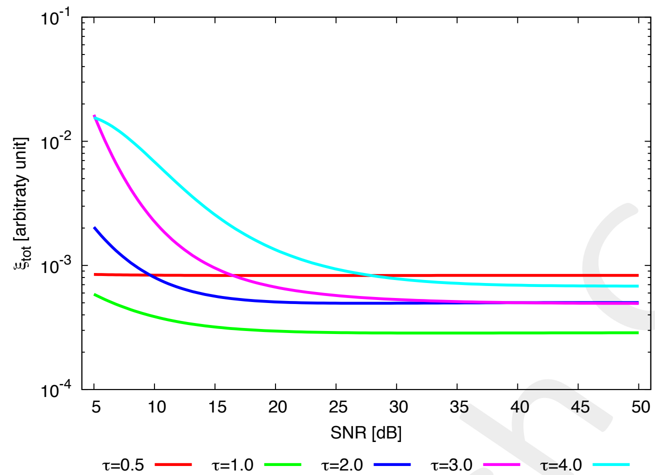

(a)

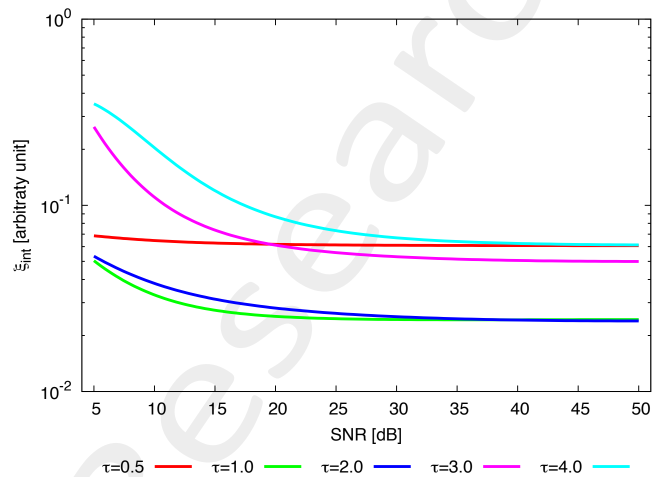

(b)

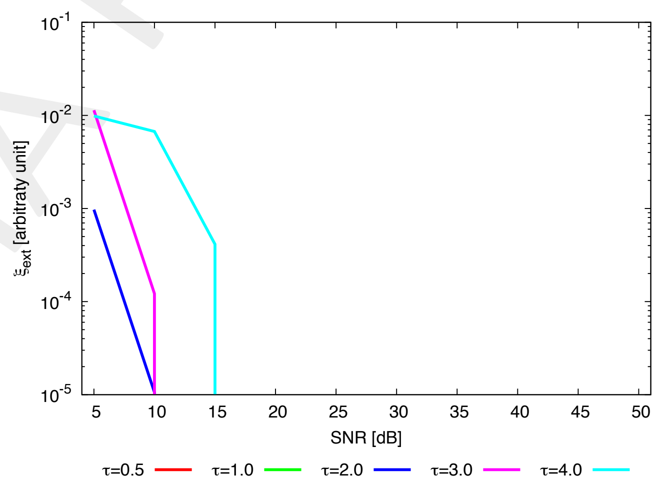

(c)

Figure 10. Behaviour of error figures as a function of SNR, for different ε_r values: (a) total error ξ_{tot}, (b) internal error ξ_{int}, (c) external error ξ_{ext}.

2.1.2 Two Strips of Sides $l_1 = 0.16\lambda$, $l_2 = 0.50\lambda$

Goal: show the performances of the multi-frequency $MT - BCS$ when dealing with a sparse scatterer

- Number of frequencies F
- Number of Views: V
- Number of Measurements: M
- Number of Cells for the Inversion: N
- Number of Cells for the Direct solver: D
- Side of the investigation domain: L

Test Case Description

Direct solver:

- Square domain divided in $\sqrt{D} \times \sqrt{D}$ cells
- Domain side: $L = 3\lambda$ (at the central frequency)
- $D = 1296$ (discretization for the direct solver: $< \lambda/10$)

Investigation domain:

- Square domain divided in $\sqrt{N} \times \sqrt{N}$ cells
- $L = 3\lambda$
- $2ka = 2 \times \frac{2\pi}{\lambda} \times \frac{L\sqrt{2}}{2} = 6\pi\sqrt{2} = 26.65$
- $\#DOF = \frac{(2ka)^2}{2} = \frac{(2\times\frac{2\pi}{\lambda}\times\frac{L\sqrt{2}}{2})^2}{2} = 4\pi^2\left(\frac{L}{\lambda}\right)^2 = 4\pi^2 \times 9 \approx 355.3$
- N scelto in modo da essere vicino a $\#DOF$: $N = 324$ (18×18)

Measurement domain:

- Measurement points taken on a circle of radius $\rho = 3\lambda$ (at the central frequency)
- $M \approx 2ka \rightarrow M = 27$

Sources:

- $V = 1$ $(\theta = 0°)$
- Amplitude: $A = 1$ (plane waves)
- Number of Frequencies: $F = 11$
- Frequency Range: $I_F = [150\,Mhz\,:\,450MHz]$ - Frequency Step: $S_F = [30\,Mhz]$

Object:

- Two strips of sides $l_1 = 0.16\lambda$, $l_2 = 0.50\lambda$
- $\varepsilon_r = \in \{1.5, 2.0, 2.5, 3.0, 3.5, 4.0, 4.5, 5.0\}$
- $\sigma = 0$ [S/m]

MT-BCS parameters:

- Gamma prior on noise variance parameters: $\beta_1 = 6.5 \times 10^{-1}$, $\beta_2 = 5.8 \times 10^{-2}$
- Convergenze parameter: $\tau = 1.0 \times 10^{-8}$

Two Homogeneous Strips of Sides $l_1 = 0.16\lambda$, $l_2 = 0.50\lambda$ - Reconstruction Profiles

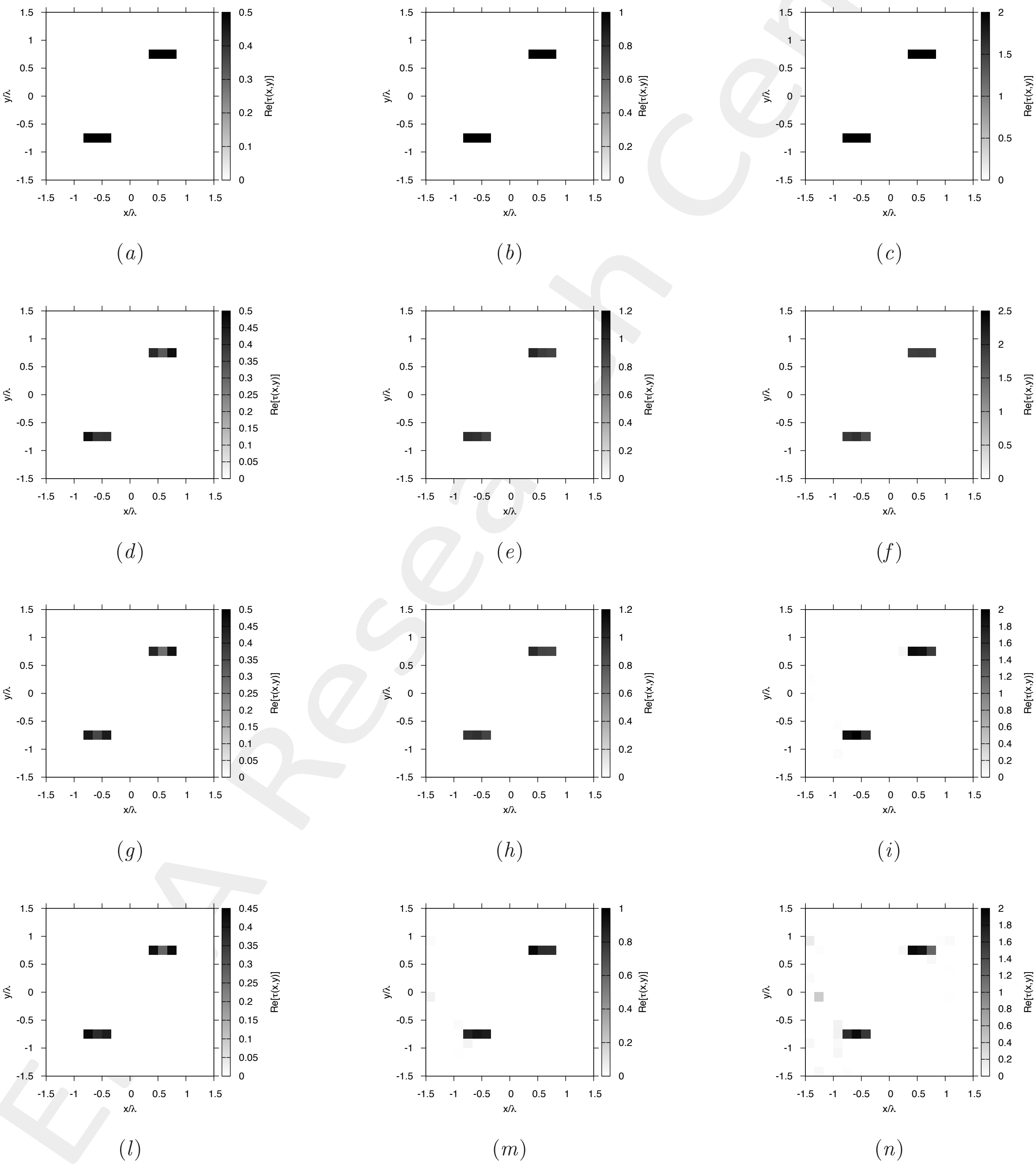

Figure 11. Actual object $(a)(b)(c)$ and MF-MT-BCS reconstructed object with $\varepsilon_r = 1.5$ $(d)(g)(l)$, $\varepsilon_r = 2.0$ $(e)(h)(m)$, and $\varepsilon_r = 3.0$ $(f)(i)(n)$, for $SNR = 20$ [dB] $(d)(e)(f)$, $SNR = 10$ [dB] $(g)(h)(i)$ and $SNR = 5$ [dB] $(l)(m)(n)$.

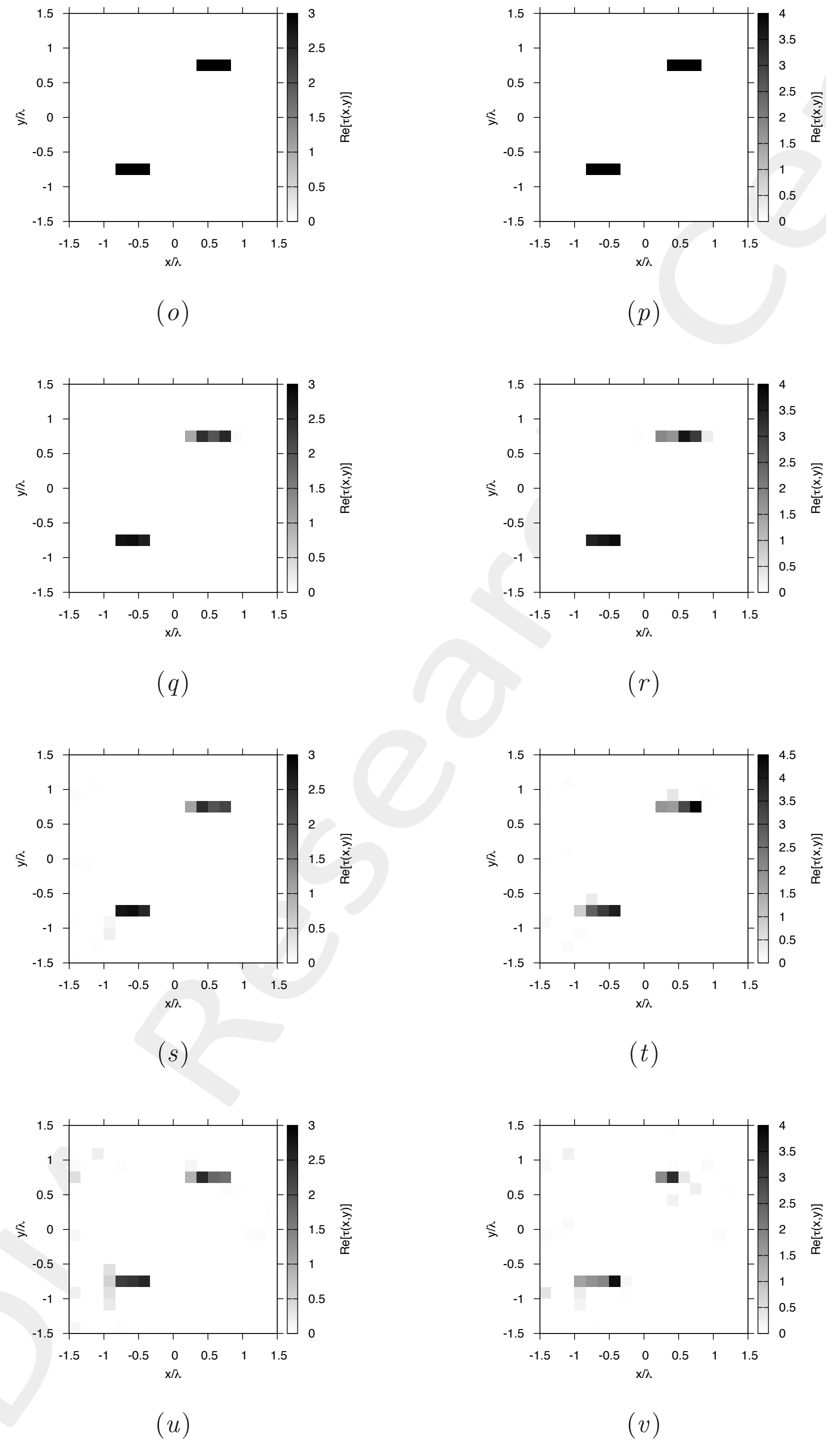

Figure 11. Actual object $(o)(p)$ and MF-MT-BCS reconstructed object with $\varepsilon_r = 4.0$ $(q)(s)(u)$, $\varepsilon_r = 5.0$ $(r)(t)(v)$, for $SNR = 20$ [dB] $(q)(r)$, $SNR = 10$ [dB] $(s)(t)$ and $SNR = 5$ [dB] $(u)(v)$.

Two Homogeneous Strips of Sides $l_1 = 0.16\lambda$, $l_2 = 0.50\lambda$ - Error Figures vs. ε_r

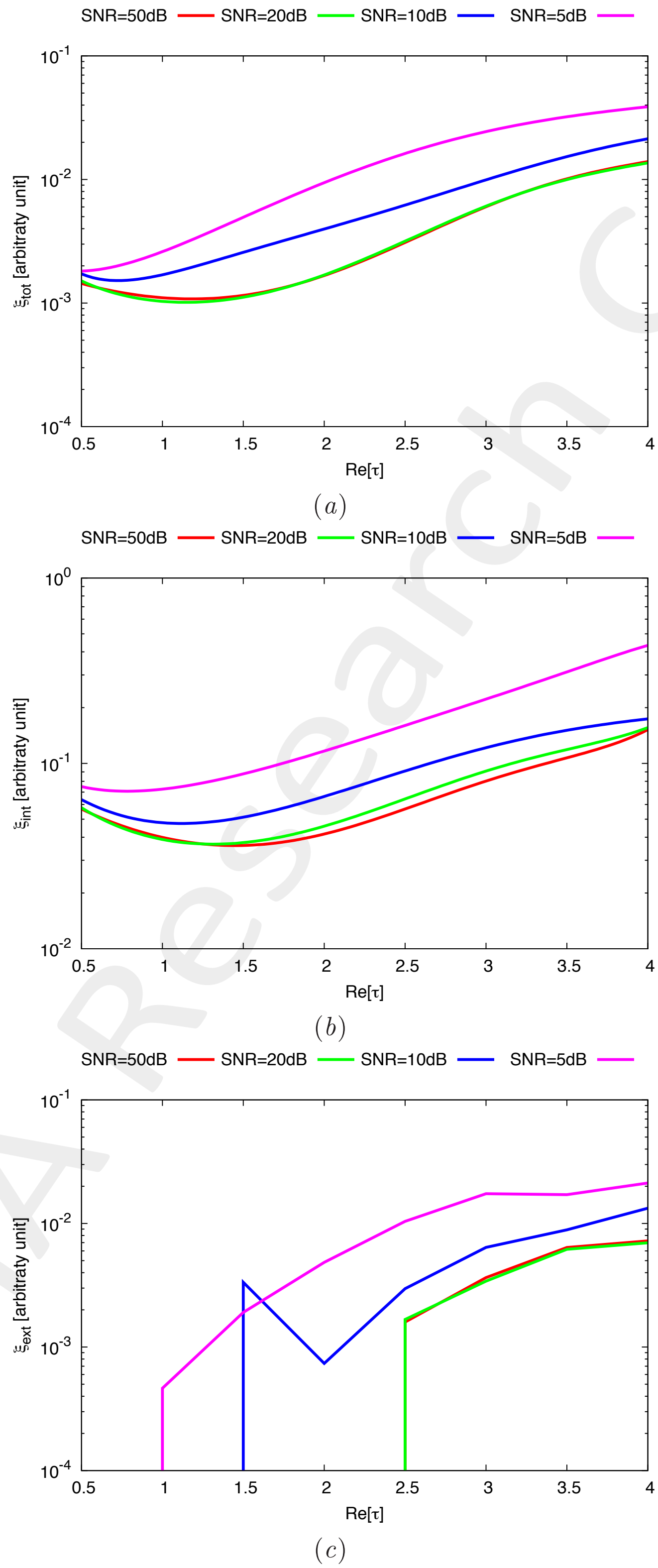

Figure 12. Behaviour of error figures as a function of ε_r, for different SNR values: (a) total error ξ_{tot}, (b) internal error ξ_{int}, (c) external error ξ_{ext}.

Two Homogeneous Strip of Sides $l_1 = 0.16\lambda$, $l_2 = 0.50\lambda$ - Error Figures vs. SNR

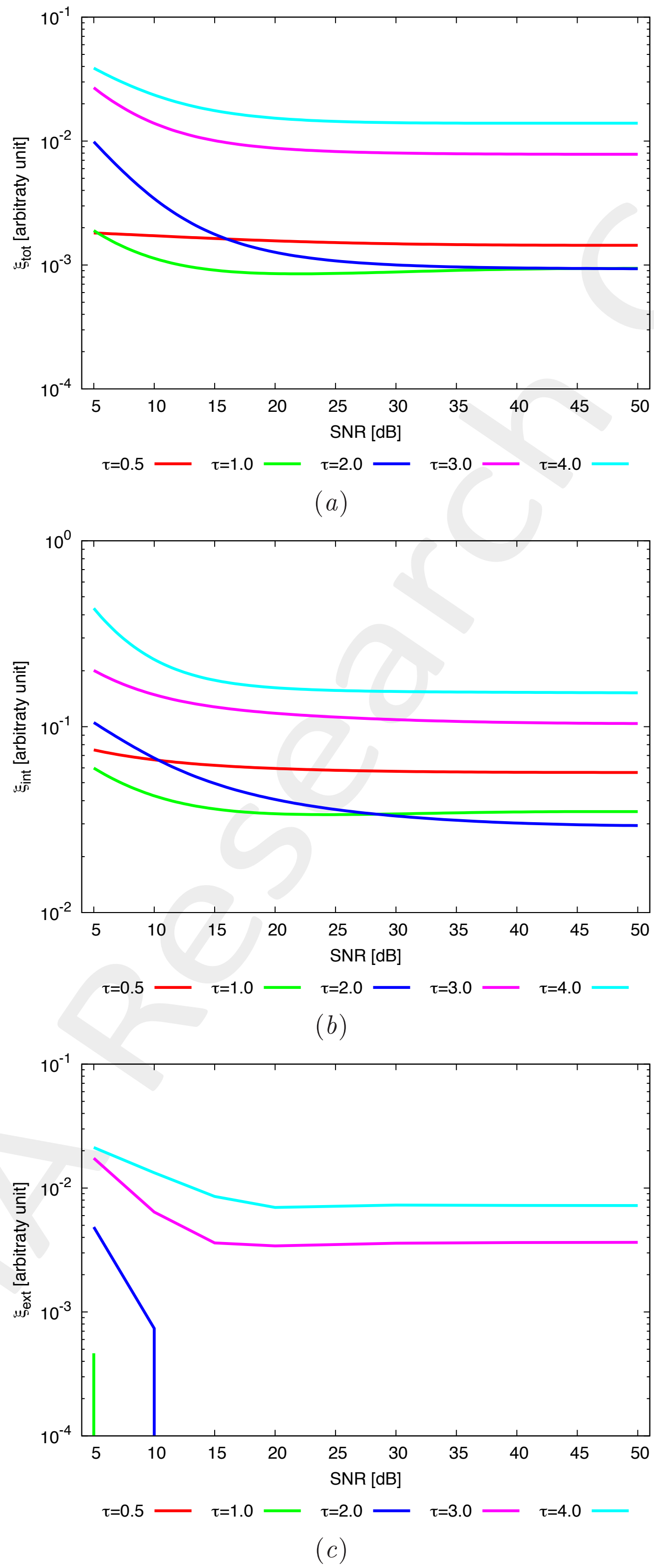

Figure 13. Behaviour of error figures as a function of SNR, for different ε_r values: (a) total error ξ_{tot}, (b) internal error ξ_{int}, (c) external error ξ_{ext}.

2.1.3 Eight Pixels of Side $l = 0.16\lambda$

Goal: show the performances of the multi-frequency $MT - BCS$ when dealing with a sparse scatterer

- Number of frequencies F
- Number of Views: V
- Number of Measurements: M
- Number of Cells for the Inversion: N
- Number of Cells for the Direct solver: D
- Side of the investigation domain: L

Test Case Description

Direct solver:

- Square domain divided in $\sqrt{D} \times \sqrt{D}$ cells
- Domain side: $L = 3\lambda$ (at the central frequency)
- $D = 1296$ (discretization for the direct solver: $< \lambda/10$)

Investigation domain:

- Square domain divided in $\sqrt{N} \times \sqrt{N}$ cells
- $L = 3\lambda$
- $2ka = 2 \times \frac{2\pi}{\lambda} \times \frac{L\sqrt{2}}{2} = 6\pi\sqrt{2} = 26.65$
- $\#DOF = \frac{(2ka)^2}{2} = \frac{(2\times\frac{2\pi}{\lambda}\times\frac{L\sqrt{2}}{2})^2}{2} = 4\pi^2\left(\frac{L}{\lambda}\right)^2 = 4\pi^2 \times 9 \approx 355.3$
- N scelto in modo da essere vicino a $\#DOF$: $N = 324$ (18×18)

Measurement domain:

- Measurement points taken on a circle of radius $\rho = 3\lambda$ (at the central frequency)
- $M \approx 2ka \rightarrow M = 27$

Sources:

- $V = 1$ $(\theta = 0°)$
- Amplitude: $A = 1$ (plane waves)
- Number of Frequencies: $F = 11$
- Frequency Range: $I_F = [150\,Mhz \,:\, 450MHz]$ - Frequency Step: $S_F = [30\,Mhz]$

Object:

- Eight square cylinders of side $l = 0.16\lambda$
- $\varepsilon_r = \in \{1.5,\ 2.0,\ 2.5,\ 3.0,\ 3.5,\ 4.0,\ 4.5,\ 5.0\}$
- $\sigma = 0$ [S/m]

MT-BCS parameters:

- Gamma prior on noise variance parameters: $\beta_1 = 6.5 \times 10^{-1}$, $\beta_2 = 5.8 \times 10^{-2}$
- Convergenze parameter: $\tau = 1.0 \times 10^{-8}$

Eight Homogeneous Pixels of Side $l = 0.16\lambda$ - Reconstruction Profiles

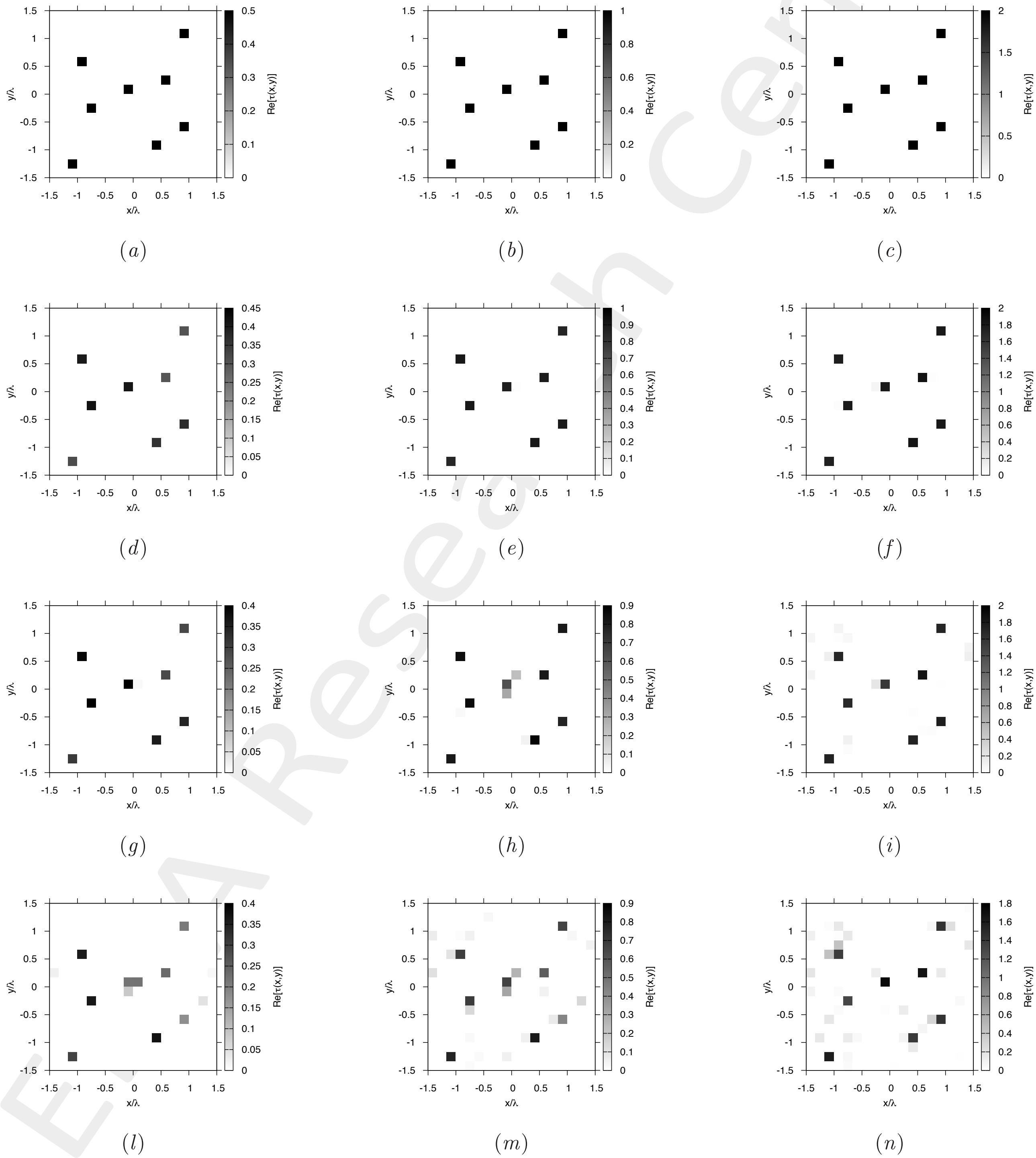

Figure 14. Actual object $(a)(b)(c)$ and MF-MT-BCS reconstructed object with $\varepsilon_r = 1.5$ $(d)(g)(l)$, $\varepsilon_r = 2.0$ $(e)(h)(m)$, and $\varepsilon_r = 3.0$ $(f)(i)(n)$, for $SNR = 20$ [dB] $(d)(e)(f)$, $SNR = 10$ [dB] $(g)(h)(i)$ and $SNR = 5$ [dB] $(l)(m)(n)$.

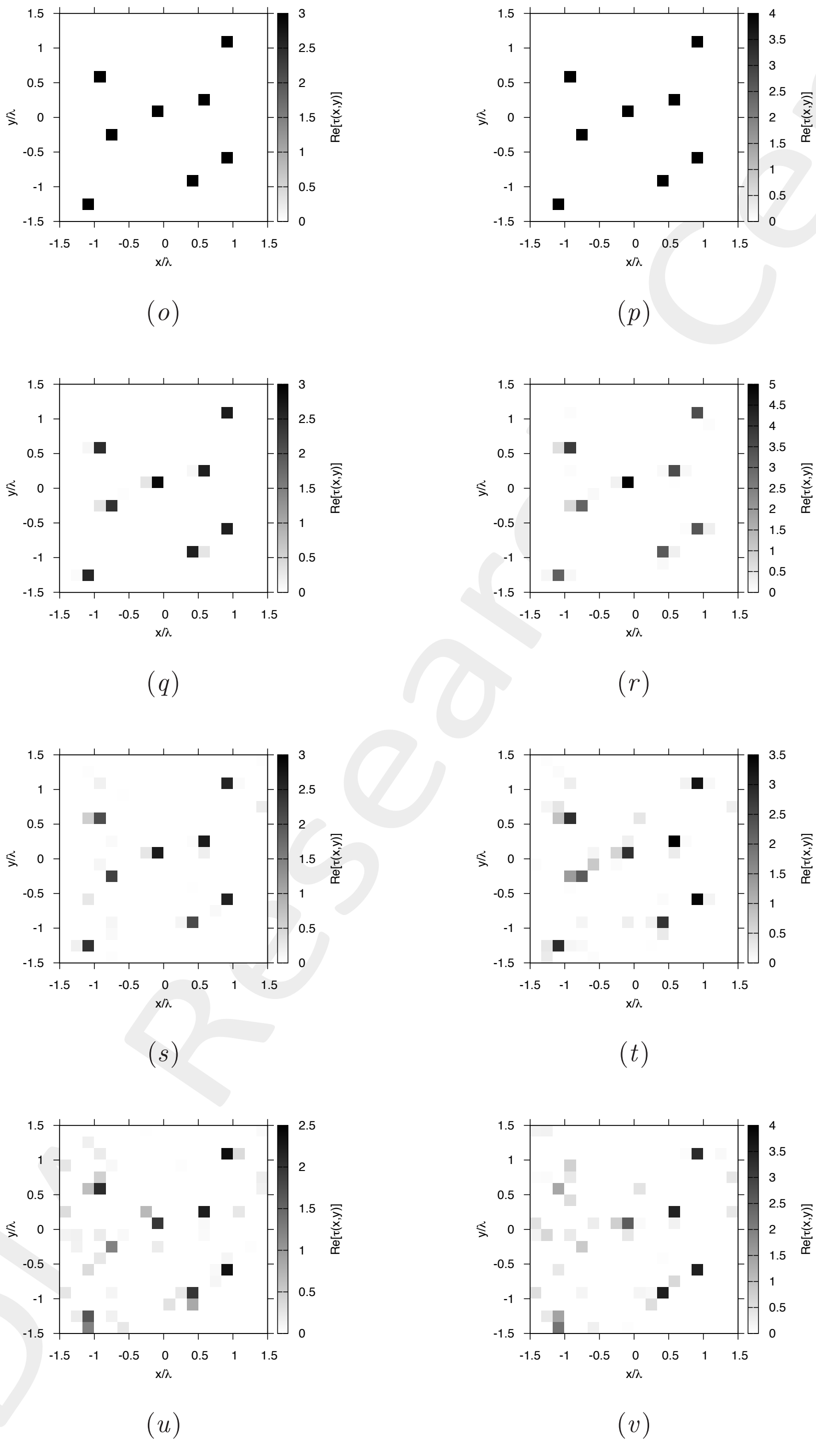

Figure 14. Actual object $(o)(p)$ and MF-MT-BCS reconstructed object with $\varepsilon_r = 4.0$ $(q)(s)(u)$, $\varepsilon_r = 5.0$ $(r)(t)(v)$, for $SNR = 20$ [dB] $(q)(r)$, $SNR = 10$ [dB] $(s)(t)$ and $SNR = 5$ [dB] $(u)(v)$.

Eight Homogeneous Pixels of Side $l = 0.16\lambda$ - Error Figures vs. ε_r

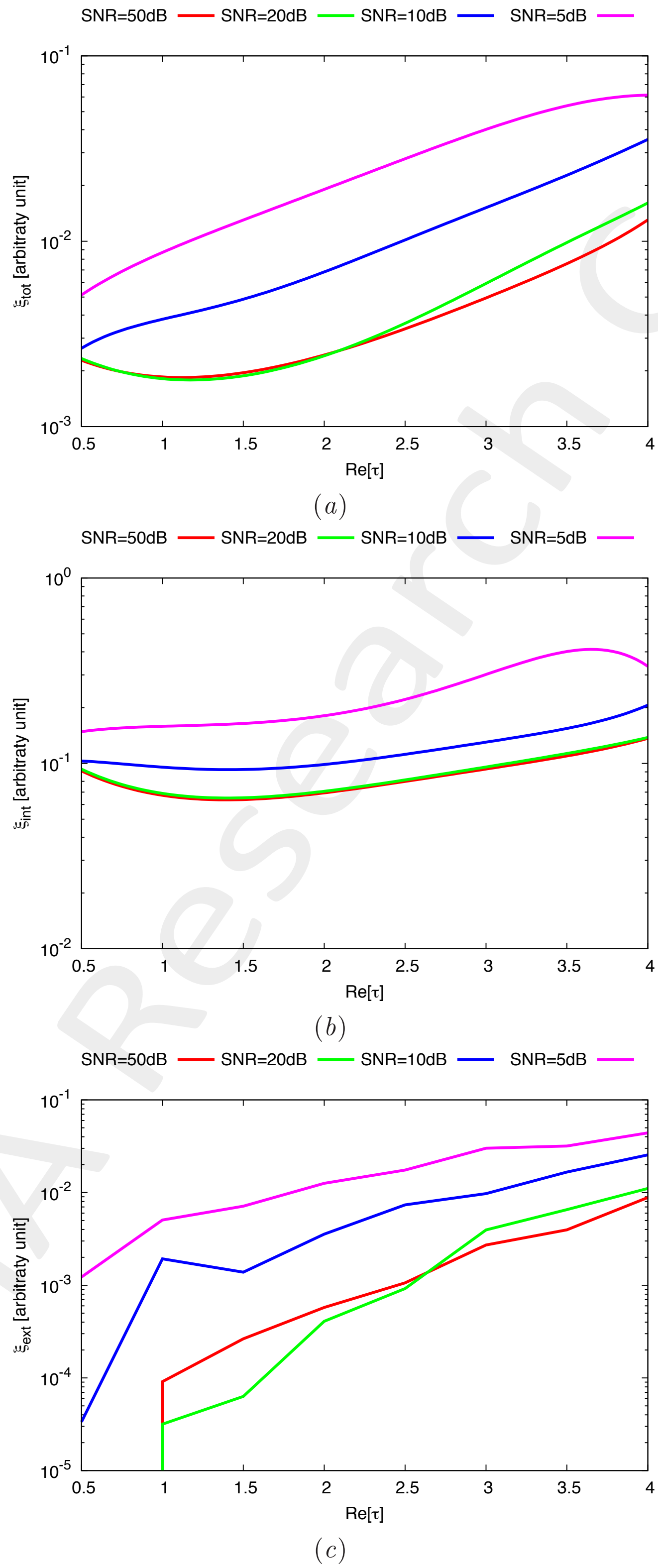

(a) (b) (c)

Figure 15. Behaviour of error figures as a function of ε_r, for different SNR values: (a) total error ξ_{tot}, (b) internal error ξ_{int}, (c) external error ξ_{ext}.

Eight Homogeneous Pixels of Side $l = 0.16\lambda$ - Error Figures vs. SNR

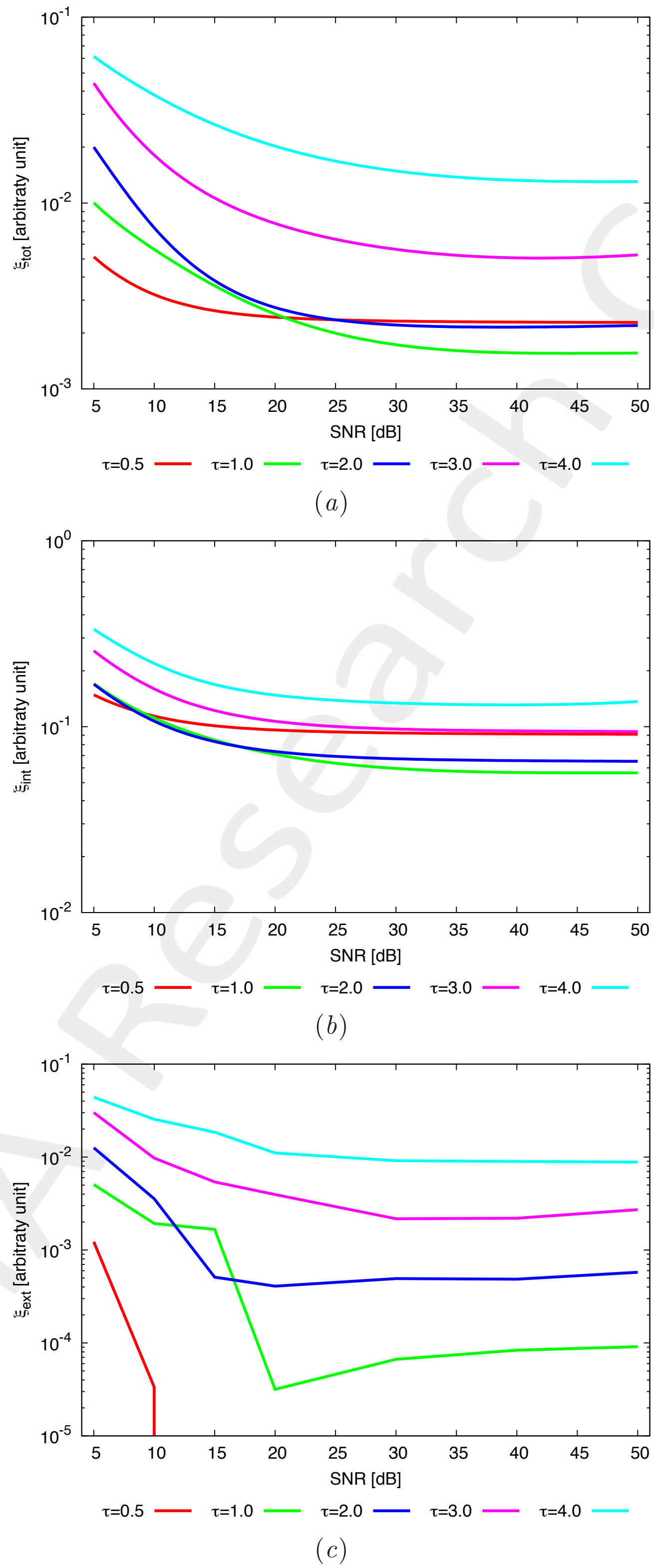

Figure 16. Behaviour of error figures as a function of SNR, for different ε_r values: (a) total error ξ_{tot}, (b) internal error ξ_{int}, (c) external error ξ_{ext}.

2.1.4 Three Objects of Different Shapes

Goal: show the performances of the multi-frequency $MT - BCS$ when dealing with a sparse scatterer

- Number of frequencies F
- Number of Views: V
- Number of Measurements: M
- Number of Cells for the Inversion: N
- Number of Cells for the Direct solver: D
- Side of the investigation domain: L

Test Case Description

Direct solver:

- Square domain divided in $\sqrt{D} \times \sqrt{D}$ cells
- Domain side: $L = 3\lambda$ (at the central frequency)
- $D = 1296$ (discretization for the direct solver: $< \lambda/10$)

Investigation domain:

- Square domain divided in $\sqrt{N} \times \sqrt{N}$ cells
- $L = 3\lambda$
- $2ka = 2 \times \frac{2\pi}{\lambda} \times \frac{L\sqrt{2}}{2} = 6\pi\sqrt{2} = 26.65$
- $\#DOF = \frac{(2ka)^2}{2} = \frac{(2\times\frac{2\pi}{\lambda}\times\frac{L\sqrt{2}}{2})^2}{2} = 4\pi^2 \left(\frac{L}{\lambda}\right)^2 = 4\pi^2 \times 9 \approx 355.3$
- N scelto in modo da essere vicino a $\#DOF$: $N = 324$ (18×18)

Measurement domain:

- Measurement points taken on a circle of radius $\rho = 3\lambda$ (at the central frequency)
- $M \approx 2ka \rightarrow M = 27$

Sources:

- $V = 1$ $(\theta = 0°)$
- Amplitude: $A = 1$ (plane waves)
- Number of Frequencies: $F = 11$
- Frequency Range: $I_F = [150\,Mhz\,:\,450MHz]$ - Frequency Step: $S_F = [30\,Mhz]$

Object:

- Strip of sides $l_1^{obj_1} = 0.16\lambda$, $l_2^{obj_1} = 0.50\lambda$; Square cylinder of side $l^{obj_2} = 0.33\lambda$; L-shaped cylinder
- $\varepsilon_r = \in \{1.5, 2.0, 2.5, 3.0, 3.5, 4.0, 4.5, 5.0\}$
- $\sigma = 0$ [S/m]

MT-BCS parameters:

- Gamma prior on noise variance parameters: $\beta_1 = 6.5 \times 10^{-1}$, $\beta_2 = 5.8 \times 10^{-2}$
- Convergenze parameter: $\tau = 1.0 \times 10^{-8}$

Three Homogeneous Objects of Different Shapes - Reconstruction Profiles

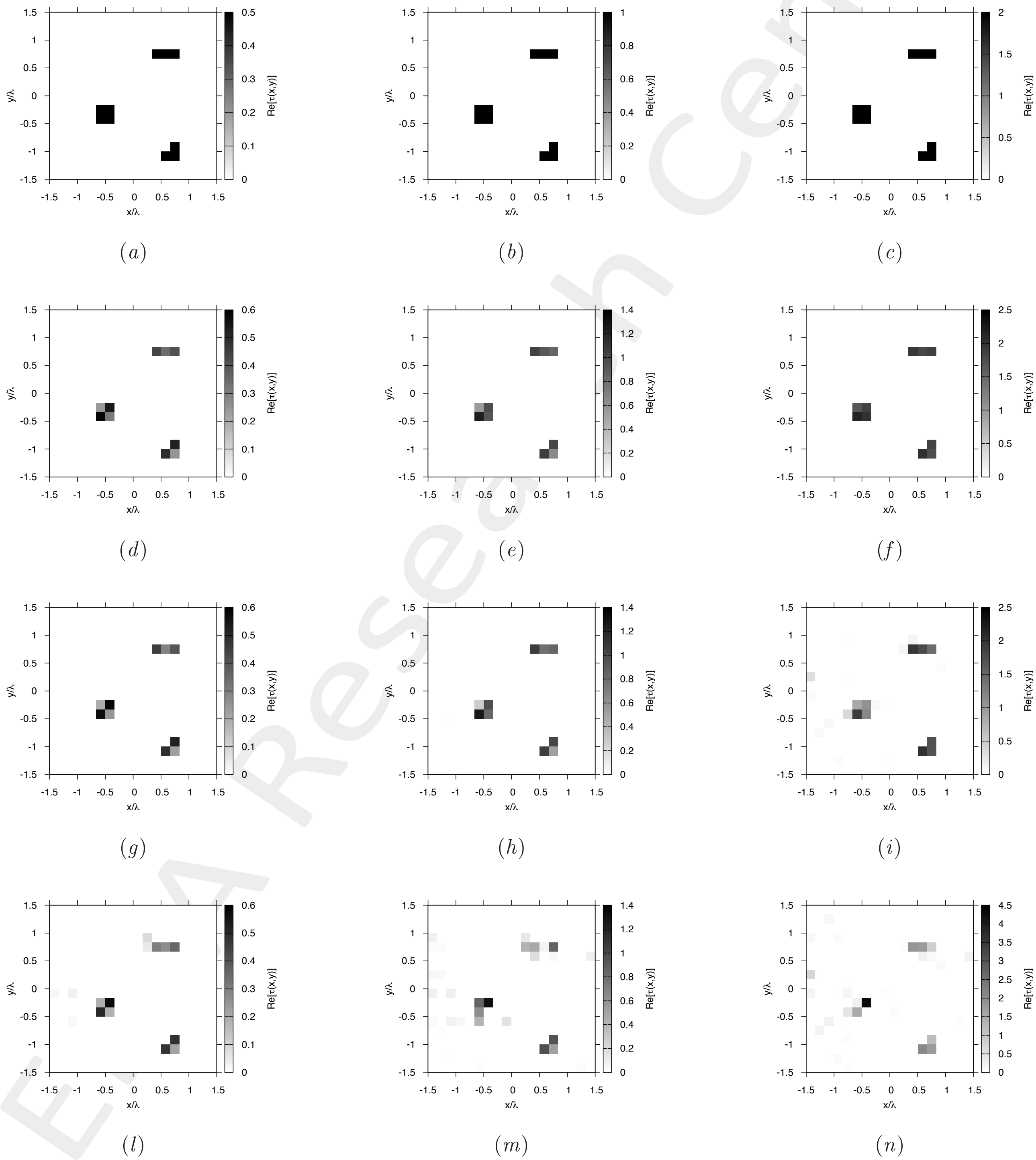

Figure 17. Actual object $(a)(b)(c)$ and MF-MT-BCS reconstructed object with $\varepsilon_r = 1.5$ $(d)(g)(l)$, $\varepsilon_r = 2.0$ $(e)(h)(m)$, and $\varepsilon_r = 3.0$ $(f)(i)(n)$, for $SNR = 20$ [dB] $(d)(e)(f)$, $SNR = 10$ [dB] $(g)(h)(i)$ and $SNR = 5$ [dB] $(l)(m)(n)$.

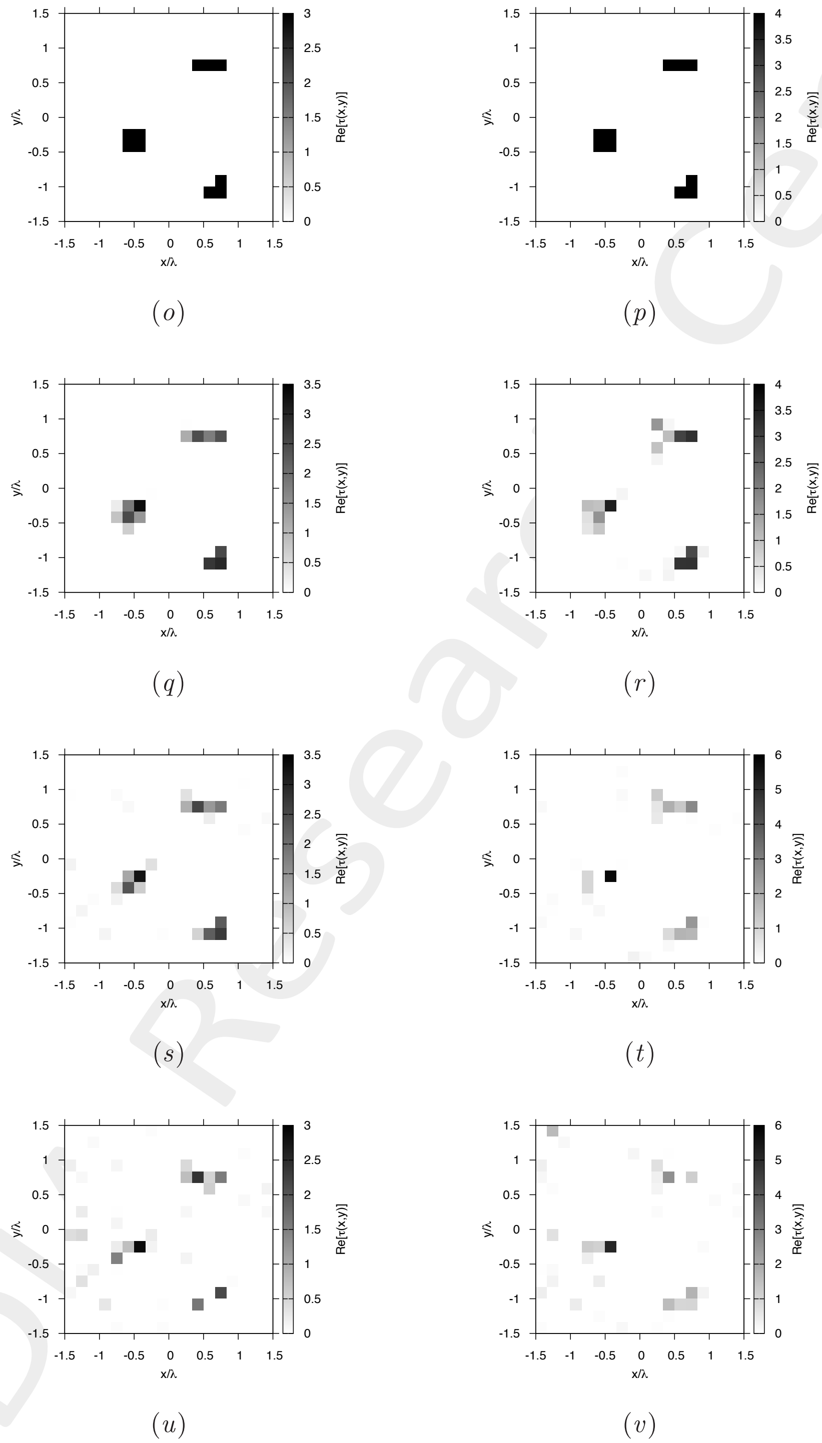

Figure 17. Actual object $(o)(p)$ and MF-MT-BCS reconstructed object with $\varepsilon_r = 4.0$ $(q)(s)(u)$, $\varepsilon_r = 5.0$ $(r)(t)(v)$, for $SNR = 20$ [dB] $(q)(r)$, $SNR = 10$ [dB] $(s)(t)$ and $SNR = 5$ [dB] $(u)(v)$.

Three Homogeneous Objects of Different Shapes - Error Figures vs. ε_r

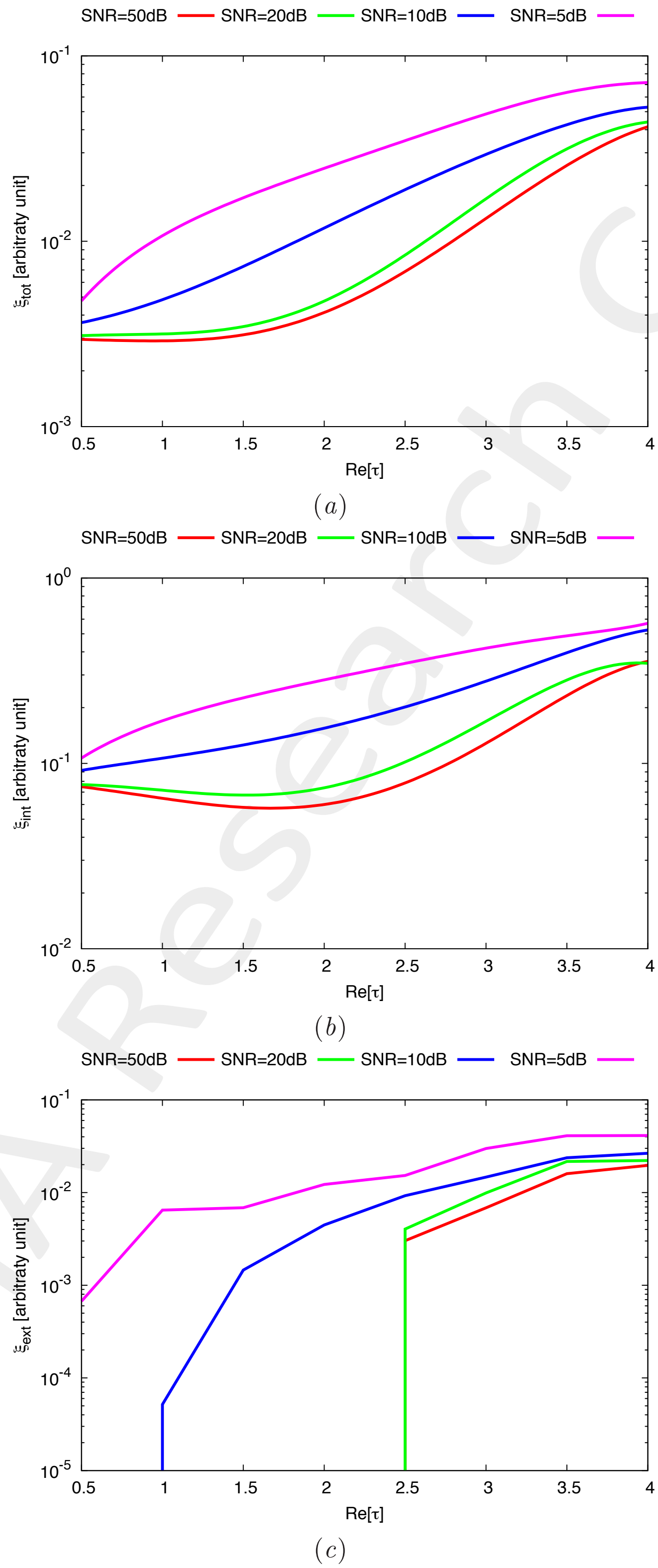

Figure 18. Behaviour of error figures as a function of ε_r, for different SNR values: (a) total error ξ_{tot}, (b) internal error ξ_{int}, (c) external error ξ_{ext}.

Three Homogeneous Objects of Different Shapes - Error Figures vs. SNR

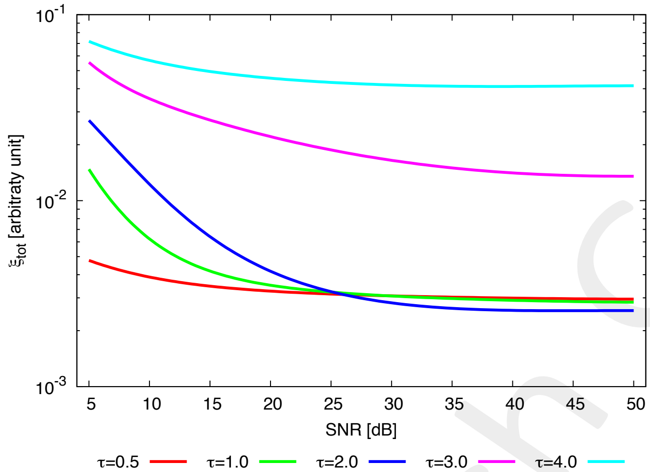

(a)

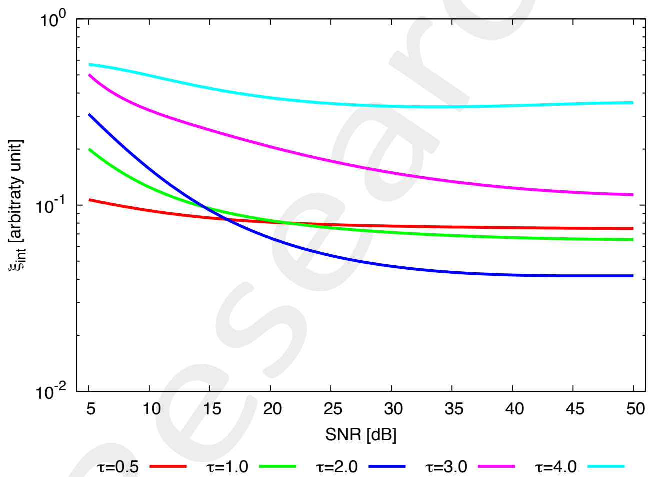

(b)

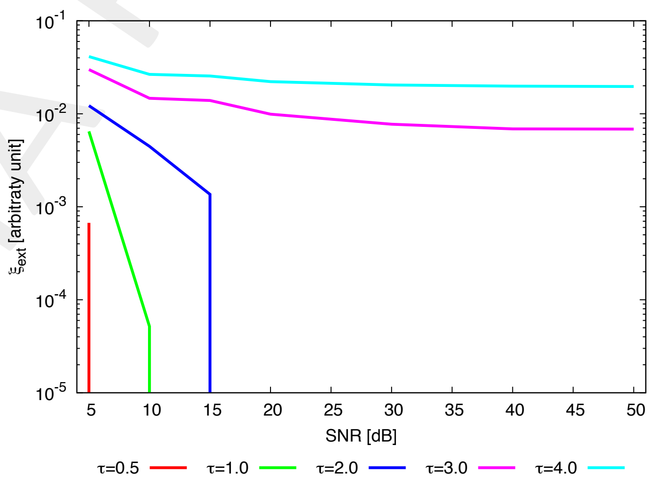

(c)

Figure 19. Behaviour of error figures as a function of SNR, for different ε_r values: (a) total error ξ_{tot}, (b) internal error ξ_{int}, (c) external error ξ_{ext}.

2.1.5 Rectangle of Sides $l_1 = 0.66\lambda$, $l_2 = 0.33\lambda$

Goal: show the performances of the multi-frequency $MT - BCS$ when dealing with a sparse scatterer

- Number of frequencies F
- Number of Views: V
- Number of Measurements: M
- Number of Cells for the Inversion: N
- Number of Cells for the Direct solver: D
- Side of the investigation domain: L

Test Case Description

Direct solver:

- Square domain divided in $\sqrt{D} \times \sqrt{D}$ cells
- Domain side: $L = 3\lambda$ (at the central frequency)
- $D = 1296$ (discretization for the direct solver: $< \lambda/10$)

Investigation domain:

- Square domain divided in $\sqrt{N} \times \sqrt{N}$ cells
- $L = 3\lambda$
- $2ka = 2 \times \frac{2\pi}{\lambda} \times \frac{L\sqrt{2}}{2} = 6\pi\sqrt{2} = 26.65$
- $\#DOF = \frac{(2ka)^2}{2} = \frac{(2\times\frac{2\pi}{\lambda}\times\frac{L\sqrt{2}}{2})^2}{2} = 4\pi^2\left(\frac{L}{\lambda}\right)^2 = 4\pi^2 \times 9 \approx 355.3$
- N scelto in modo da essere vicino a $\#DOF$: $N = 324$ (18×18)

Measurement domain:

- Measurement points taken on a circle of radius $\rho = 3\lambda$ (at the central frequency)
- $M \approx 2ka \rightarrow M = 27$

Sources:

- $V = 1$ $(\theta = 0°)$
- Amplitude: $A = 1$ (plane waves)
- Number of Frequencies: $F = 11$
- Frequency Range: $I_F = [150\, Mhz\, :\, 450 MHz]$ - Frequency Step: $S_F = [30\, Mhz]$

Object:

- Rectangle of sides $l_1 = 0.33\lambda$, $l_2 = 0.66\lambda$
- $\varepsilon_r = \in \{1.5,\, 2.0,\, 2.5,\, 3.0,\, 3.5,\, 4.0,\, 4.5,\, 5.0\}$
- $\sigma = 0$ [S/m]

MT-BCS parameters:

- Gamma prior on noise variance parameters: $\beta_1 = 6.5 \times 10^{-1}$, $\beta_2 = 5.8 \times 10^{-2}$
- Convergenze parameter: $\tau = 1.0 \times 10^{-8}$

Homogeneous Rectangle of Sides $l_1 = 0.66\lambda$, $l_2 = 0.33\lambda$ - Reconstruction Profiles

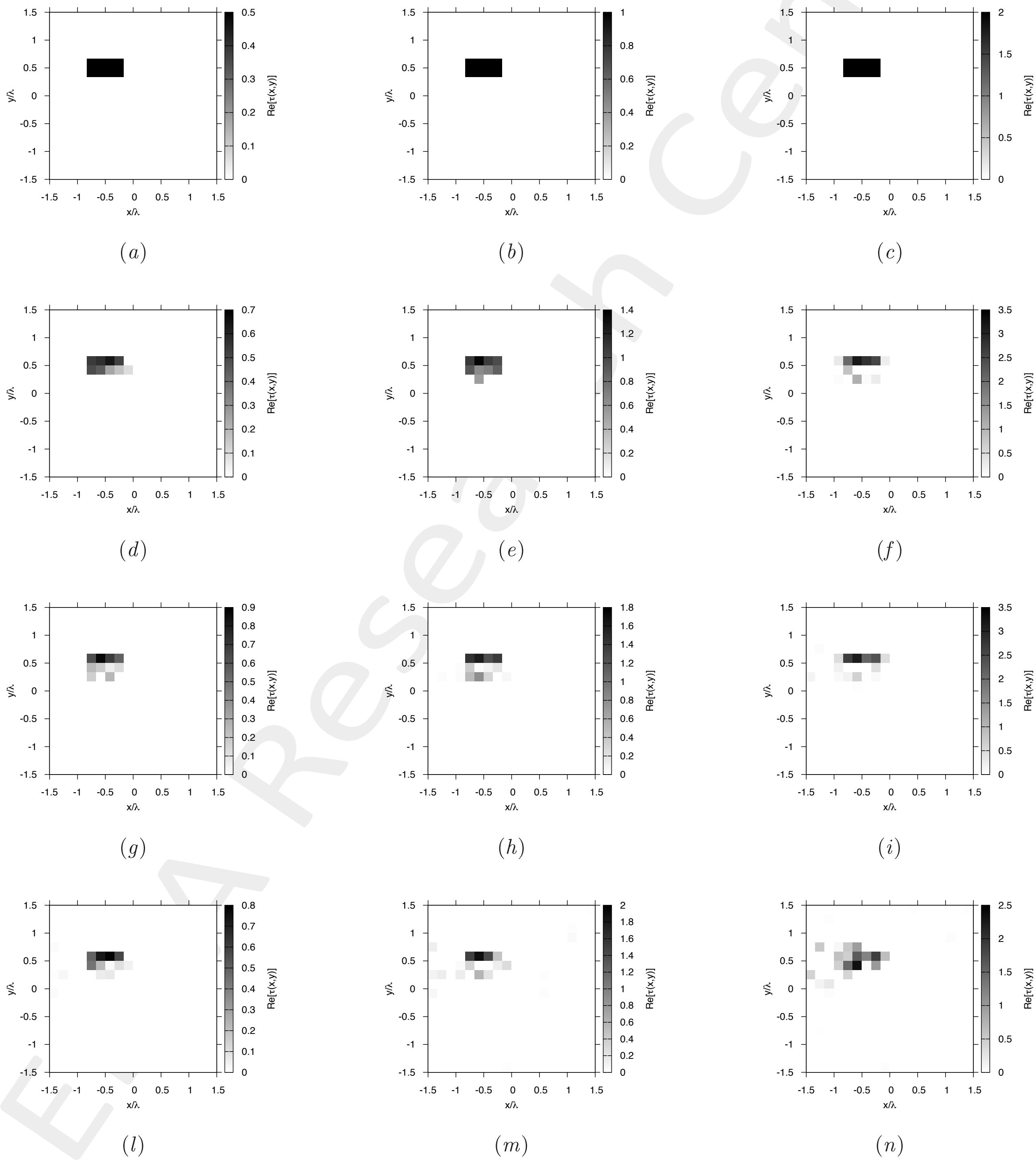

Figure 20. Actual object $(a)(b)(c)$ and MF-MT-BCS reconstructed object with $\varepsilon_r = 1.5$ $(d)(g)(l)$, $\varepsilon_r = 2.0$ $(e)(h)(m)$, and $\varepsilon_r = 3.0$ $(f)(i)(n)$, for $SNR = 20$ [dB] $(d)(e)(f)$, $SNR = 10$ [dB] $(g)(h)(i)$ and $SNR = 5$ [dB] $(l)(m)(n)$.

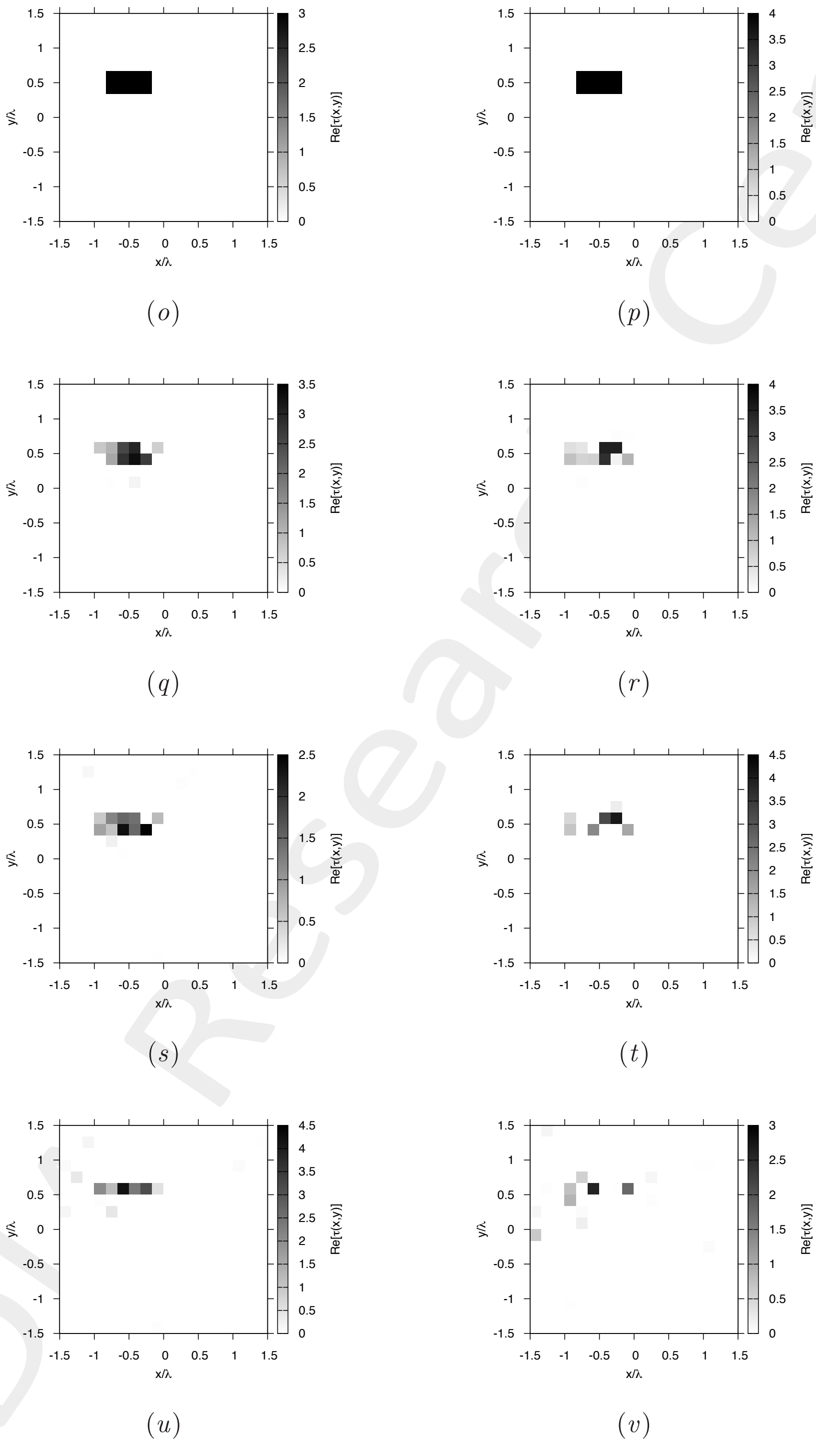

Figure 20. Actual object $(o)(p)$ and MF-MT-BCS reconstructed object with $\varepsilon_r = 4.0$ $(q)(s)(u)$, $\varepsilon_r = 5.0$ $(r)(t)(v)$, for $SNR = 20$ [dB] $(q)(r)$, $SNR = 10$ [dB] $(s)(t)$ and $SNR = 5$ [dB] $(u)(v)$.

Homogeneous Rectangle of Sides $l_1 = 0.66\lambda$, $l_2 = 0.33\lambda$ - Error Figures vs. ε_r

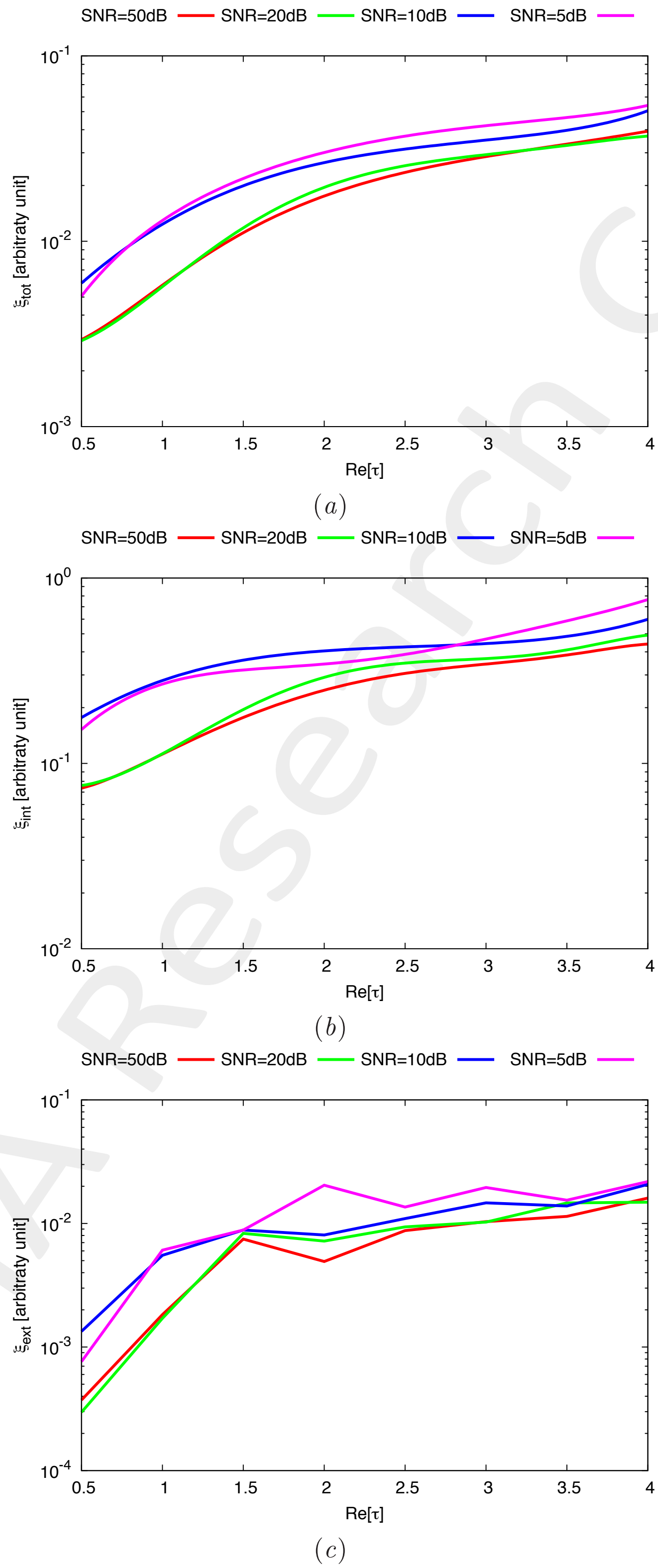

Figure 21. Behaviour of error figures as a function of ε_r, for different SNR values: (a) total error ξ_{tot}, (b) internal error ξ_{int}, (c) external error ξ_{ext}.

Homogeneous Rectangle of Sides $l_1 = 0.66\lambda$, $l_2 = 0.33\lambda$ - Error Figures vs. SNR

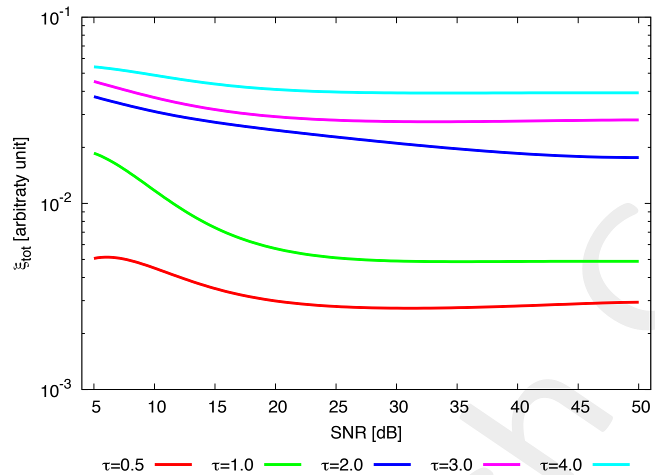

(a)

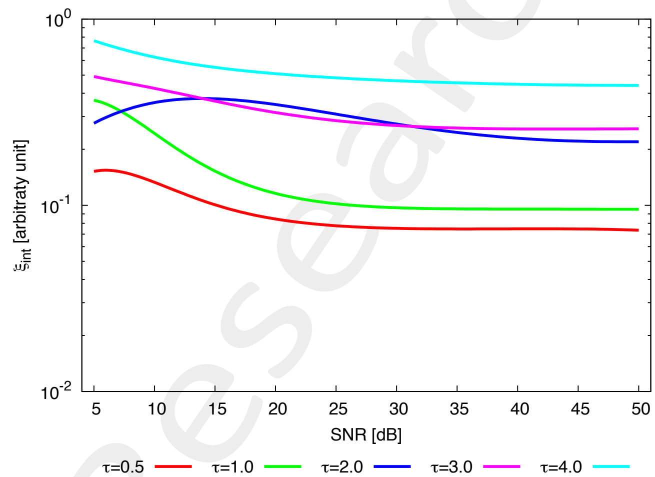

(b)

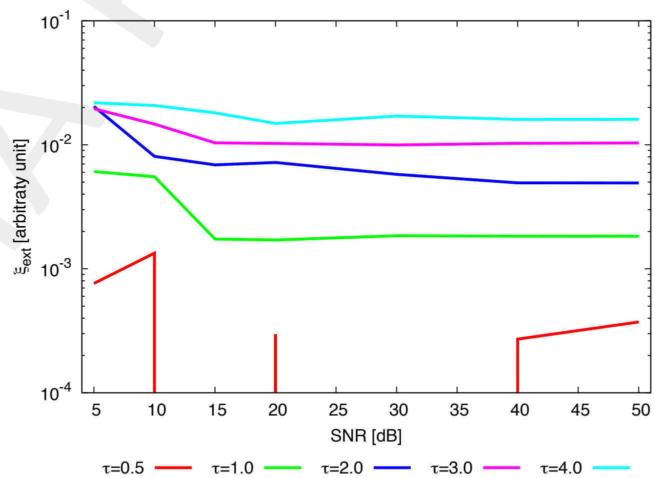

(c)

Figure 22. Behaviour of error figures as a function of SNR, for different ε_r values: (a) total error ξ_{tot}, (b) internal error ξ_{int}, (c) external error ξ_{ext}.

2.1.6 Rectangle of Sides $l_1 = 0.66\lambda$, $l_2 = 0.33\lambda$ and Square of Side $l = 0.33\lambda$

Goal: show the performances of the multi-frequency $MT - BCS$ when dealing with a sparse scatterer

- Number of frequencies F
- Number of Views: V
- Number of Measurements: M
- Number of Cells for the Inversion: N
- Number of Cells for the Direct solver: D
- Side of the investigation domain: L

Test Case Description

Direct solver:

- Square domain divided in $\sqrt{D} \times \sqrt{D}$ cells
- Domain side: $L = 3\lambda$ (at the central frequency)
- $D = 1296$ (discretization for the direct solver: $< \lambda/10$)

Investigation domain:

- Square domain divided in $\sqrt{N} \times \sqrt{N}$ cells
- $L = 3\lambda$
- $2ka = 2 \times \frac{2\pi}{\lambda} \times \frac{L\sqrt{2}}{2} = 6\pi\sqrt{2} = 26.65$
- $\#DOF = \frac{(2ka)^2}{2} = \frac{(2\times\frac{2\pi}{\lambda}\times\frac{L\sqrt{2}}{2})^2}{2} = 4\pi^2\left(\frac{L}{\lambda}\right)^2 = 4\pi^2 \times 9 \approx 355.3$
- N scelto in modo da essere vicino a $\#DOF$: $N = 324$ (18×18)

Measurement domain:

- Measurement points taken on a circle of radius $\rho = 3\lambda$ (at the central frequency)
- $M \approx 2ka \rightarrow M = 27$

Sources:

- $V = 1$ $(\theta = 0°)$
- Amplitude: $A = 1$ (plane waves)
- Number of Frequencies: $F = 11$
- Frequency Range: $I_F = [150\,Mhz\,:\,450MHz]$ - Frequency Step: $S_F = [30\,Mhz]$

Object:

- Rectangle of sides $l_1^{obj_1} = 0.33\lambda$, $l_2^{obj_1} = 0.66\lambda$; Square of sides $l^{obj_2} = 0.33\lambda$
- $\varepsilon_r = \in \{1.5, 2.0, 2.5, 3.0, 3.5, 4.0, 4.5, 5.0\}$
- $\sigma = 0$ [S/m]

MT-BCS parameters:

- Gamma prior on noise variance parameters: $\beta_1 = 6.5 \times 10^{-1}$, $\beta_2 = 5.8 \times 10^{-2}$
- Convergenze parameter: $\tau = 1.0 \times 10^{-8}$

Homogeneous Rectangle of Sides $l_1^{obj_1} = 0.66\lambda$, $l_2^{obj_1} = 0.33\lambda$ and Square of Side $l^{obj_2} = 0.33\lambda$ - Reconstruction Profiles

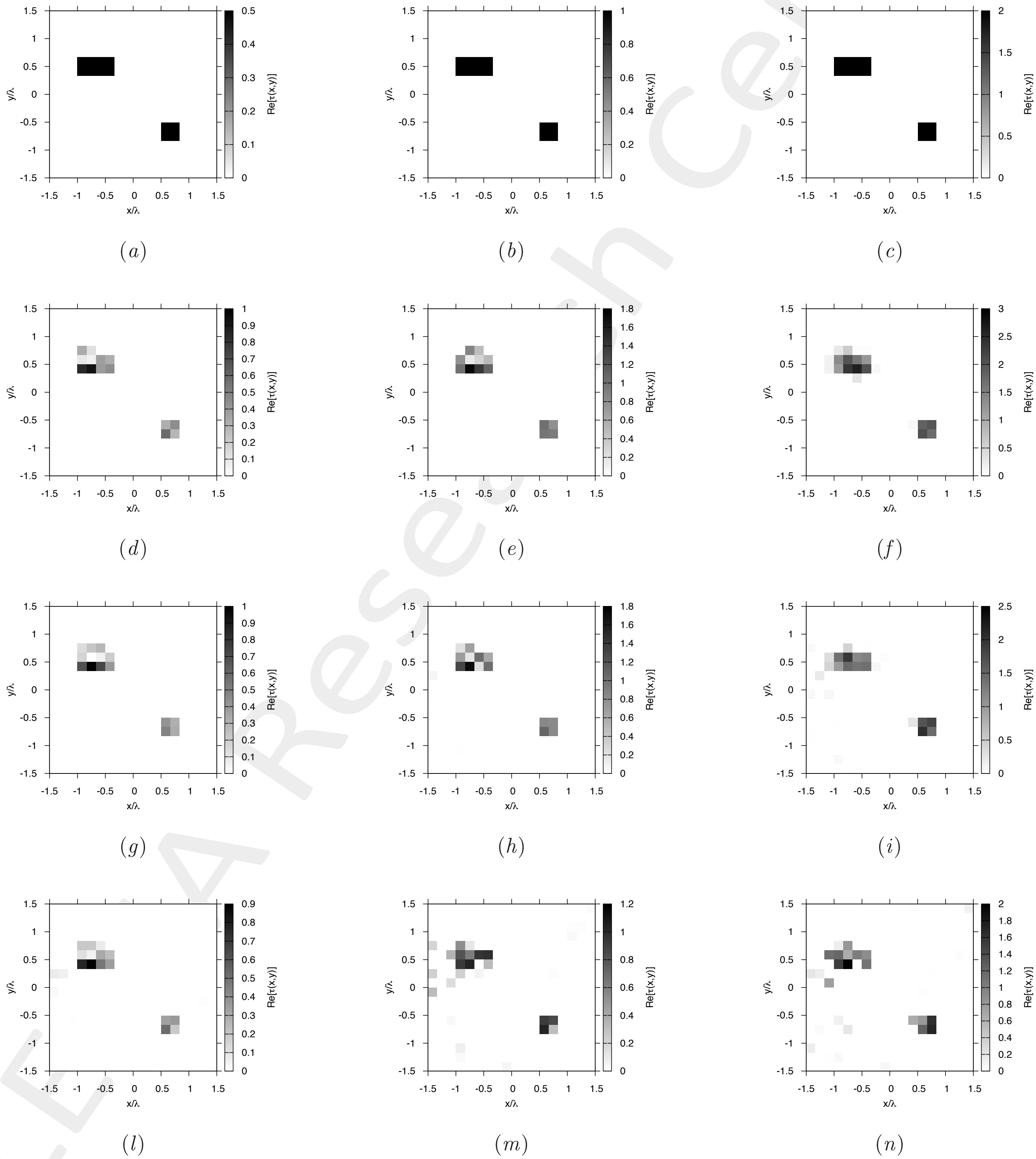

Figure 23. Actual object $(a)(b)(c)$ and MF-MT-BCS reconstructed object with $\varepsilon_r = 1.5$ $(d)(g)(l)$, $\varepsilon_r = 2.0$ $(e)(h)(m)$, and $\varepsilon_r = 3.0$ $(f)(i)(n)$, for $SNR = 20$ [dB] $(d)(e)(f)$, $SNR = 10$ [dB] $(g)(h)(i)$ and $SNR = 5$ [dB] $(l)(m)(n)$.

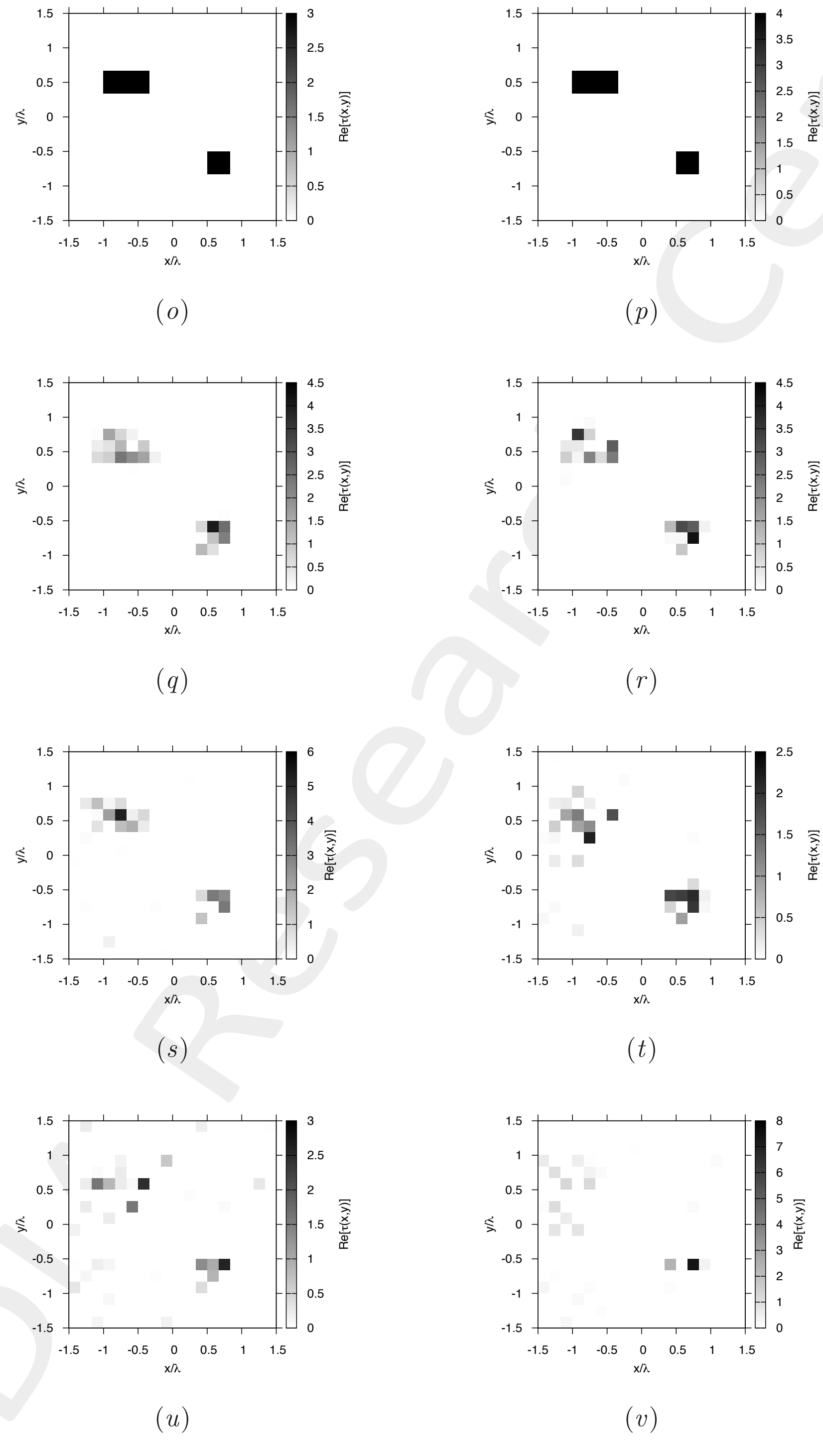

Figure 23. Actual object $(o)(p)$ and MF-MT-BCS reconstructed object with $\varepsilon_r = 4.0$ $(q)(s)(u)$, $\varepsilon_r = 5.0$ $(r)(t)(v)$, for $SNR = 20$ [dB] $(q)(r)$, $SNR = 10$ [dB] $(s)(t)$ and $SNR = 5$ [dB] $(u)(v)$.

Homogeneous Rectangle of Sides $l_1^{obj_1} = 0.66\lambda$, $l_2^{obj_1} = 0.33\lambda$ and Square of Side $l^{obj_2} = 0.33\lambda$ - Error Figures vs. ε_r

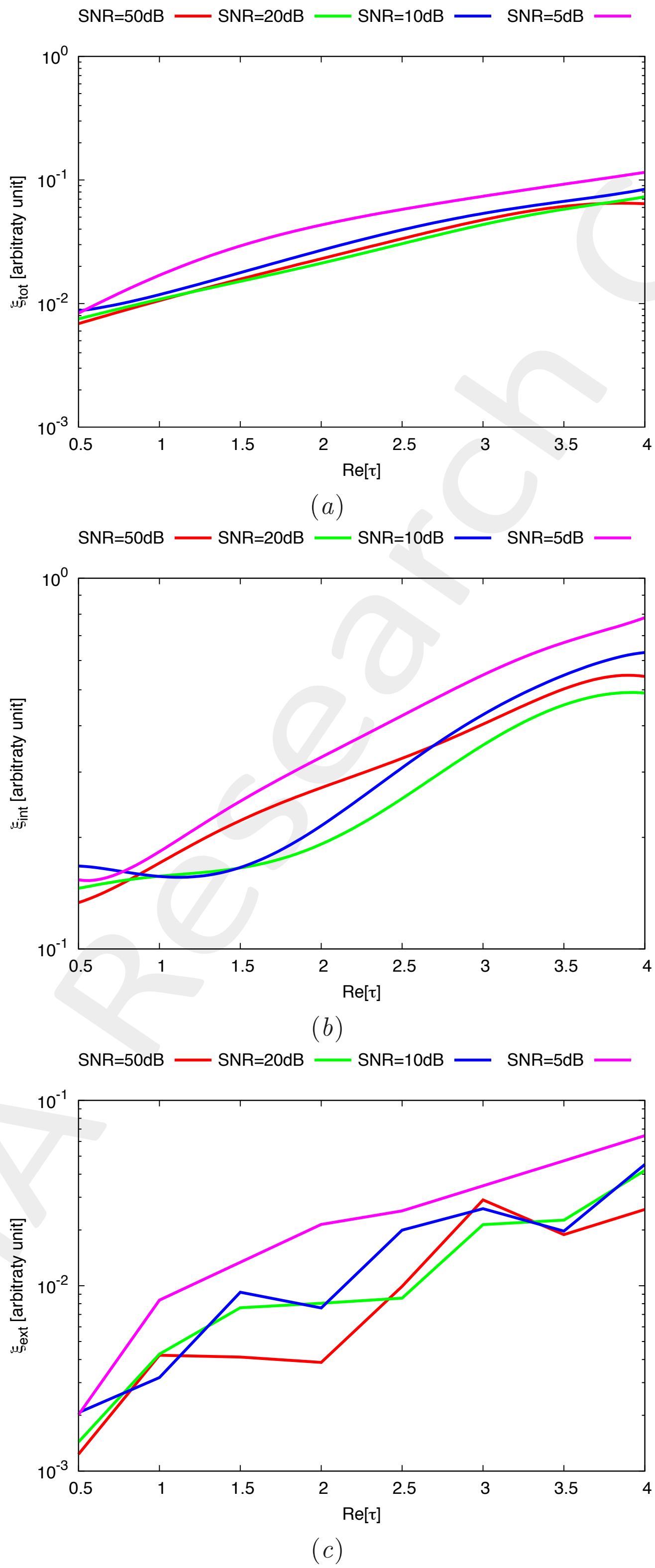

Figure 24. Behaviour of error figures as a function of ε_r, for different SNR values: (a) total error ξ_{tot}, (b) internal error ξ_{int}, (c) external error ξ_{ext}.

Homogeneous Rectangle of Sides $l_1^{obj_1} = 0.66\lambda$, $l_2^{obj_1} = 0.33\lambda$ and Square of Side $l^{obj_2} = 0.33\lambda$ - Error Figures vs. SNR

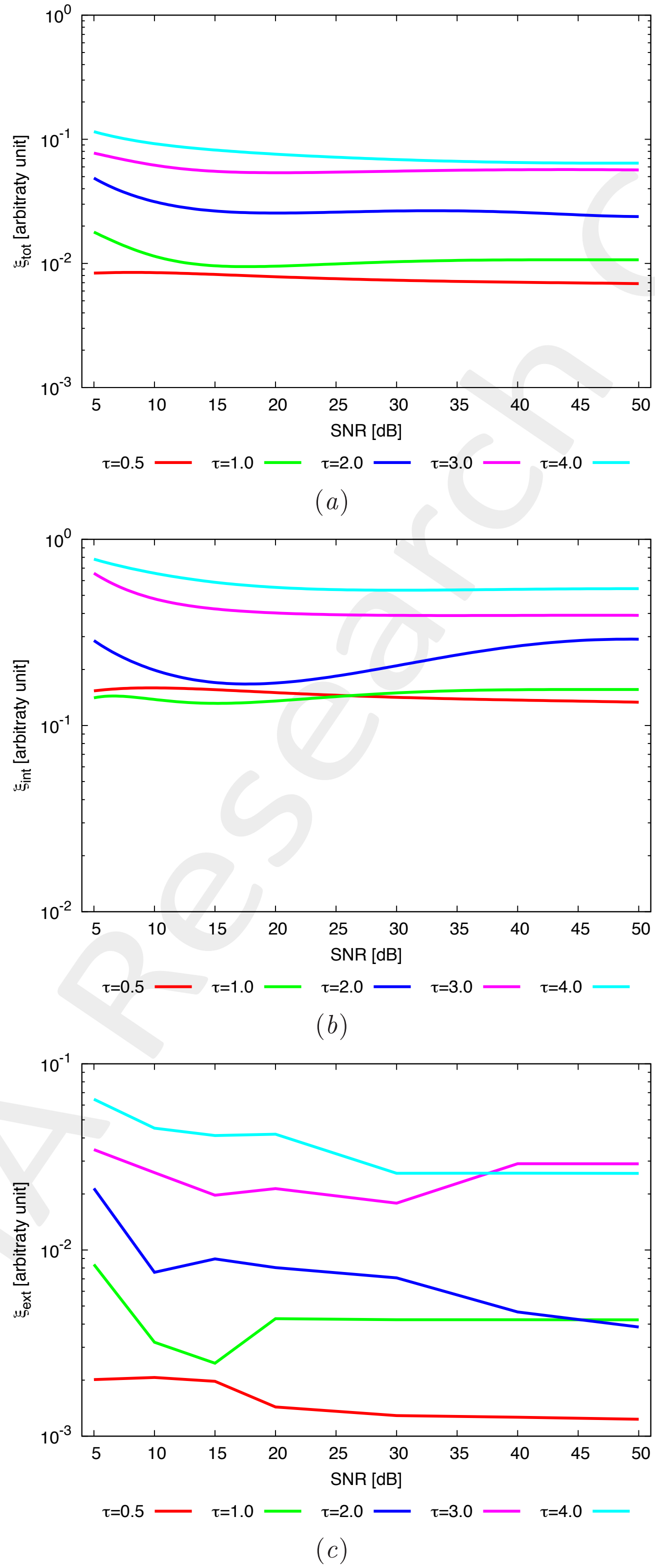

Figure 25. Behaviour of error figures as a function of SNR, for different ε_r values: (a) total error ξ_{tot}, (b) internal error ξ_{int}, (c) external error ξ_{ext}.

2.2 Non-Homogeneous Objects

2.2.1 Two Strips of Sides $l_1 = 0.16\lambda$, $l_2 = 0.50\lambda$

Goal: show the performances of the multi-frequency $MT - BCS$ when dealing with a sparse scatterer

- Number of frequencies F
- Number of Views: V
- Number of Measurements: M
- Number of Cells for the Inversion: N
- Number of Cells for the Direct solver: D
- Side of the investigation domain: L

Test Case Description

Direct solver:

- Square domain divided in $\sqrt{D} \times \sqrt{D}$ cells
- Domain side: $L = 3\lambda$ (at the central frequency)
- $D = 1296$ (discretization for the direct solver: $< \lambda/10$)

Investigation domain:

- Square domain divided in $\sqrt{N} \times \sqrt{N}$ cells
- $L = 3\lambda$
- $2ka = 2 \times \frac{2\pi}{\lambda} \times \frac{L\sqrt{2}}{2} = 6\pi\sqrt{2} = 26.65$
- $\#DOF = \frac{(2ka)^2}{2} = \frac{(2\times\frac{2\pi}{\lambda}\times\frac{L\sqrt{2}}{2})^2}{2} = 4\pi^2\left(\frac{L}{\lambda}\right)^2 = 4\pi^2 \times 9 \approx 355.3$
- N scelto in modo da essere vicino a $\#DOF$: $N = 324$ (18×18)

Measurement domain:

- Measurement points taken on a circle of radius $\rho = 3\lambda$ (at the central frequency)
- $M \approx 2ka \rightarrow M = 27$

Sources:

- $V = 1$ $(\theta = 0°)$
- Amplitude: $A = 1$ (plane waves)
- Number of Frequencies: $F = 11$
- Frequency Range: $I_F = [150\,Mhz\,:\,450MHz]$ - Frequency Step: $S_F = [30\,Mhz]$

Object:

- Two strips of sides $l_1 = 0.16\lambda$, $l_2 = 0.50\lambda$
- $\varepsilon_r^{obj_1} \in \{1.5, 2.0, 2.5, 3.0, 3.5, 4.0, 4.5, 5.0\}$, $\varepsilon_r^{obj_2} = 1.6$
- $\sigma = 0$ [S/m]

MT-BCS parameters:

- Gamma prior on noise variance parameters: $\beta_1 = 6.5 \times 10^{-1}$, $\beta_2 = 5.8 \times 10^{-2}$
- Convergenze parameter: $\tau = 1.0 \times 10^{-8}$

Two Non-Homogeneous Strips of Sides $l_1 = 0.16\lambda$, $l_2 = 0.50\lambda$ - Reconstruction Profiles

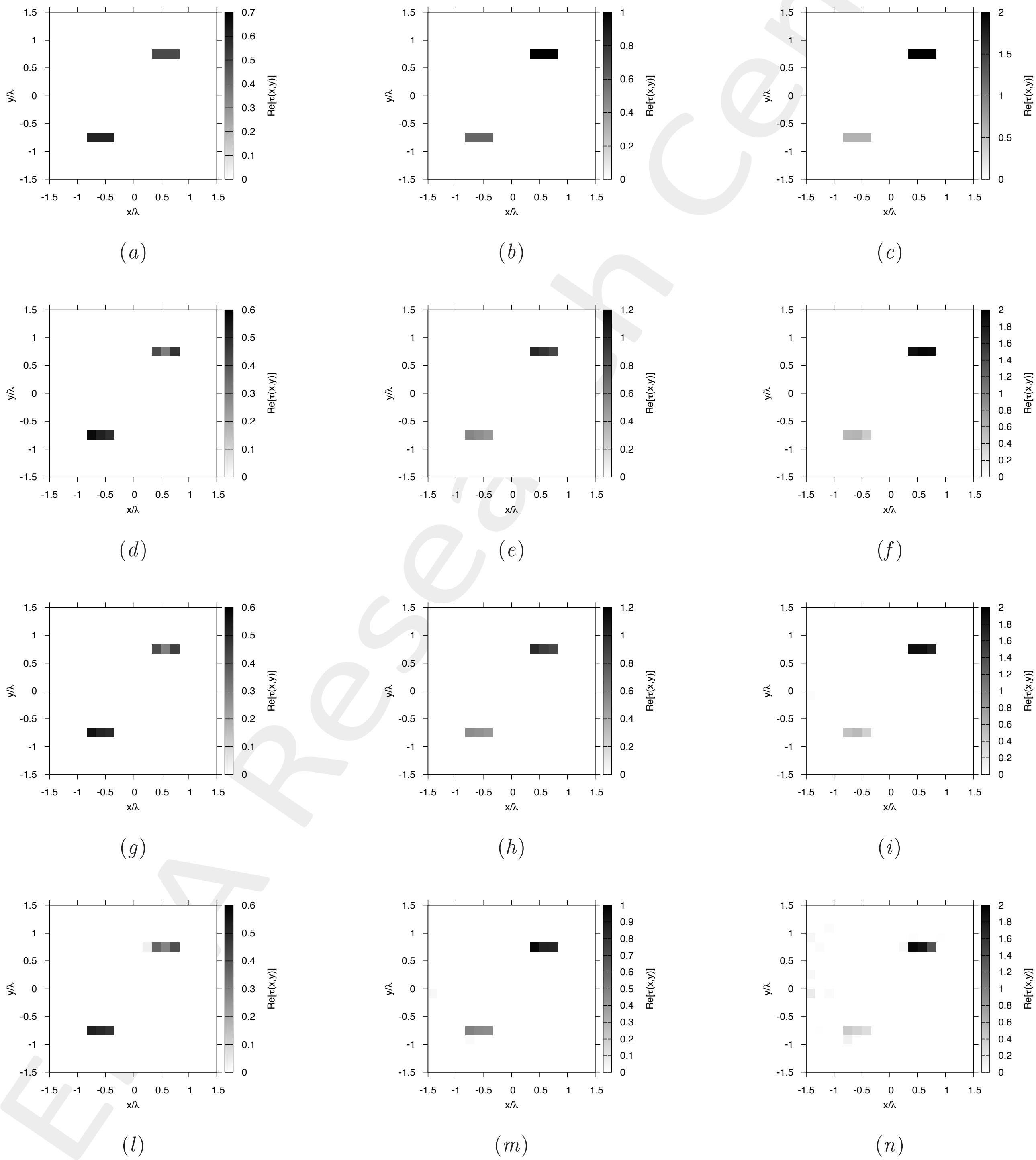

Figure 26. Actual object $(a)(b)(c)$ and MF-MT-BCS reconstructed object with $\varepsilon_r = 1.5$ $(d)(g)(l)$, $\varepsilon_r = 2.0$ $(e)(h)(m)$, and $\varepsilon_r = 3.0$ $(f)(i)(n)$, for $SNR = 20$ [dB] $(d)(e)(f)$, $SNR = 10$ [dB] $(g)(h)(i)$ and $SNR = 5$ [dB] $(l)(m)(n)$.

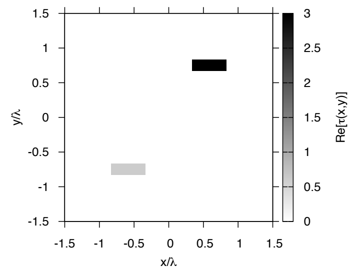

(o)

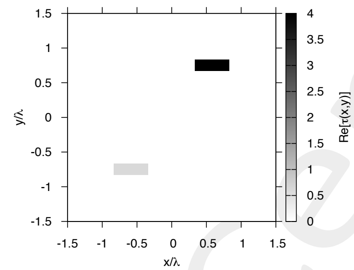

(p)

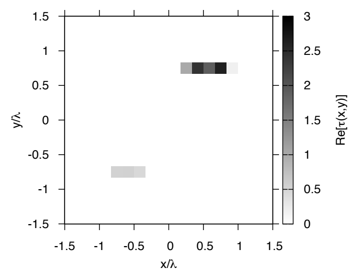

(q)

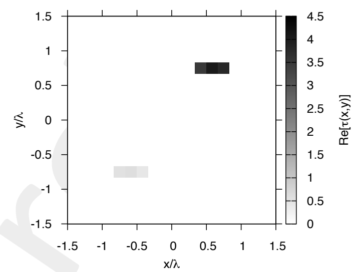

(r)

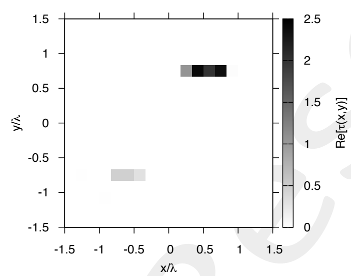

(s)

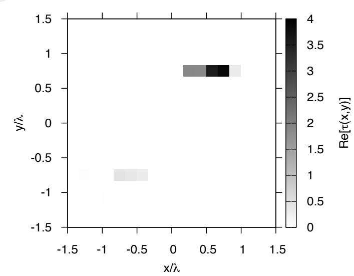

(t)

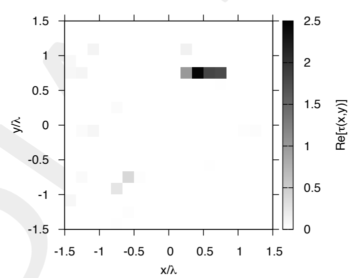

(u)

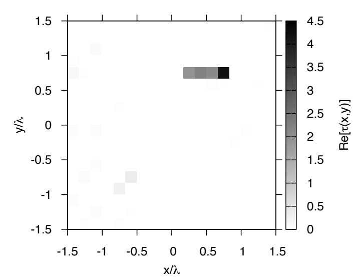

(v)

Figure 26. Actual object $(o)(p)$ and MF-MT-BCS reconstructed object with $\varepsilon_r = 4.0$ $(q)(s)(u)$, $\varepsilon_r = 5.0$ $(r)(t)(v)$, for $SNR = 20$ [dB] $(q)(r)$, $SNR = 10$ [dB] $(s)(t)$ and $SNR = 5$ [dB] $(u)(v)$.

Two Non-Homogeneous Strips of Sides $l_1 = 0.16\lambda$, $l_2 = 0.50\lambda$- Error Figures vs. ε_r

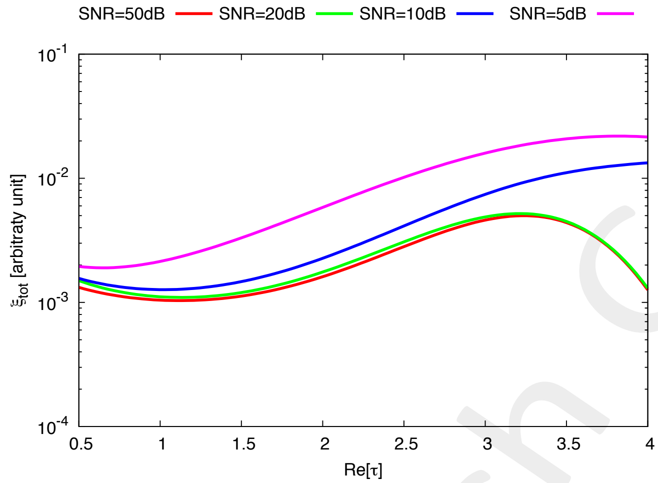

(a)

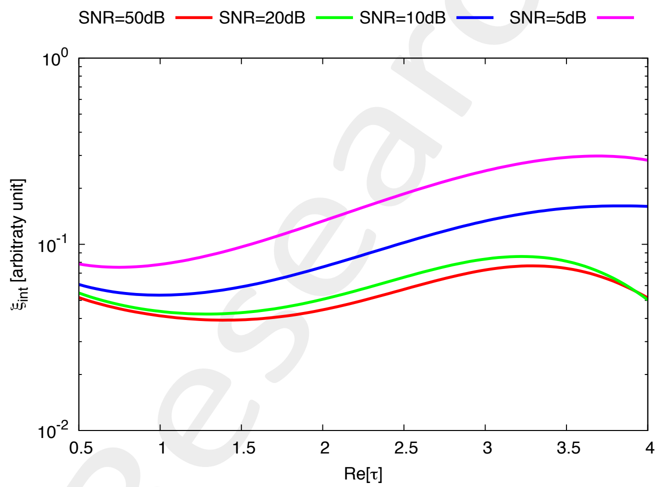

(b)

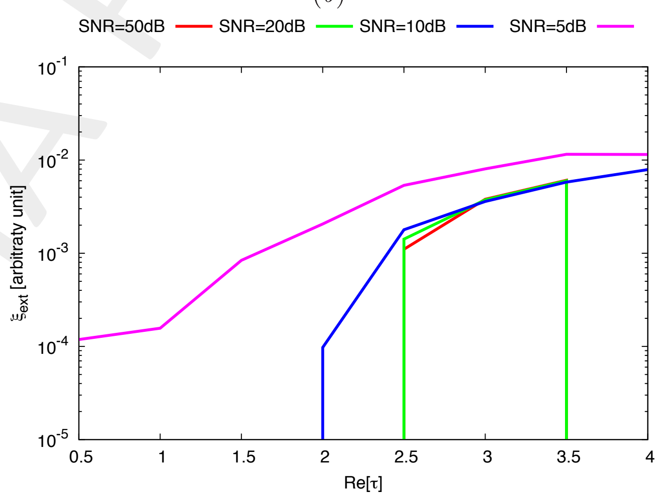

(c)

Figure 27. Behaviour of error figures as a function of ε_r, for different SNR values: (a) total error ξ_{tot}, (b) internal error ξ_{int}, (c) external error ξ_{ext}.

Two Non-Homogeneous Strips of Sides $l_1 = 0.16\lambda$, $l_2 = 0.50\lambda$- Error Figures vs. SNR

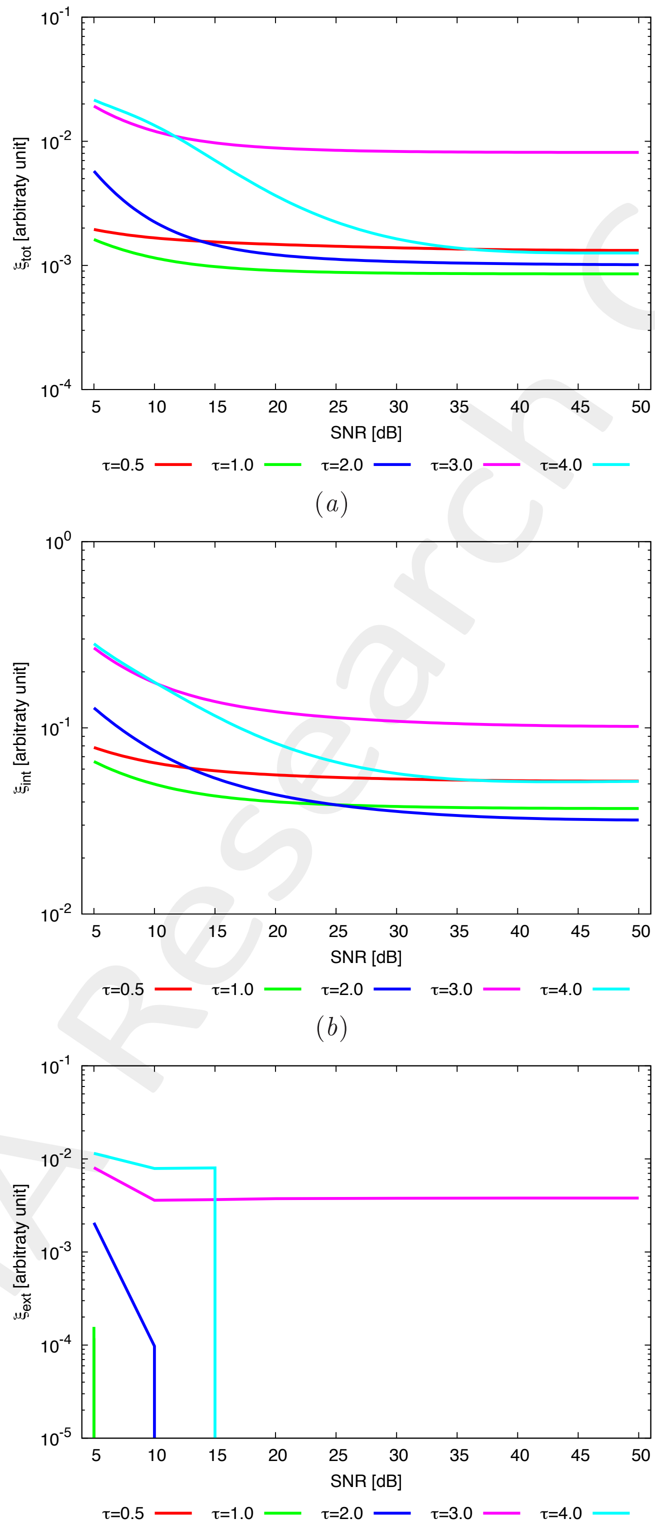

(c)

Figure 28. Behaviour of error figures as a function of SNR, for different ε_r values: (a) total error ξ_{tot}, (b) internal error ξ_{int}, (c) external error ξ_{ext}.

2.2.2 Three Objects Different Shapes

Goal: show the performances of the multi-frequency $MT - BCS$ when dealing with a sparse scatterer

- Number of frequencies F
- Number of Views: V
- Number of Measurements: M
- Number of Cells for the Inversion: N
- Number of Cells for the Direct solver: D
- Side of the investigation domain: L

Test Case Description

Direct solver:

- Square domain divided in $\sqrt{D} \times \sqrt{D}$ cells
- Domain side: $L = 3\lambda$ (at the central frequency)
- $D = 1296$ (discretization for the direct solver: $< \lambda/10$)

Investigation domain:

- Square domain divided in $\sqrt{N} \times \sqrt{N}$ cells
- $L = 3\lambda$
- $2ka = 2 \times \frac{2\pi}{\lambda} \times \frac{L\sqrt{2}}{2} = 6\pi\sqrt{2} = 26.65$
- $\#DOF = \frac{(2ka)^2}{2} = \frac{(2\times\frac{2\pi}{\lambda}\times\frac{L\sqrt{2}}{2})^2}{2} = 4\pi^2\left(\frac{L}{\lambda}\right)^2 = 4\pi^2 \times 9 \approx 355.3$
- N scelto in modo da essere vicino a $\#DOF$: $N = 324$ (18×18)

Measurement domain:

- Measurement points taken on a circle of radius $\rho = 3\lambda$ (at the central frequency)
- $M \approx 2ka \rightarrow M = 27$

Sources:

- $V = 1$ $(\theta = 0°)$
- Amplitude: $A = 1$ (plane waves)
- Number of Frequencies: $F = 11$
- Frequency Range: $I_F = [150\, Mhz\, :\, 450 MHz]$ - Frequency Step: $S_F = [30\, Mhz]$

Object:

- Strip of sides $l_1^{obj_1} = 0.16\lambda$, $l_2^{obj_1} = 0.50\lambda$; Square cylinder of side $l^{obj_2} = 0.33\lambda$; L-shaped cylinder
- $\varepsilon_r^{obj_1} = 1.6$; $\varepsilon_r^{obj_2} = \in \{1.5, 2.0, 2.5, 3.0, 3.5, 4.0, 4.5, 5.0\}$; $\varepsilon_r^{obj_3} = 2.4$
- $\sigma = 0$ [S/m]

MT-BCS parameters:

- Gamma prior on noise variance parameters: $\beta_1 = 6.5 \times 10^{-1}$, $\beta_2 = 5.8 \times 10^{-2}$
- Convergenze parameter: $\tau = 1.0 \times 10^{-8}$

Three Non-Homogeneous Objects of Different Shapes - Reconstruction Profiles

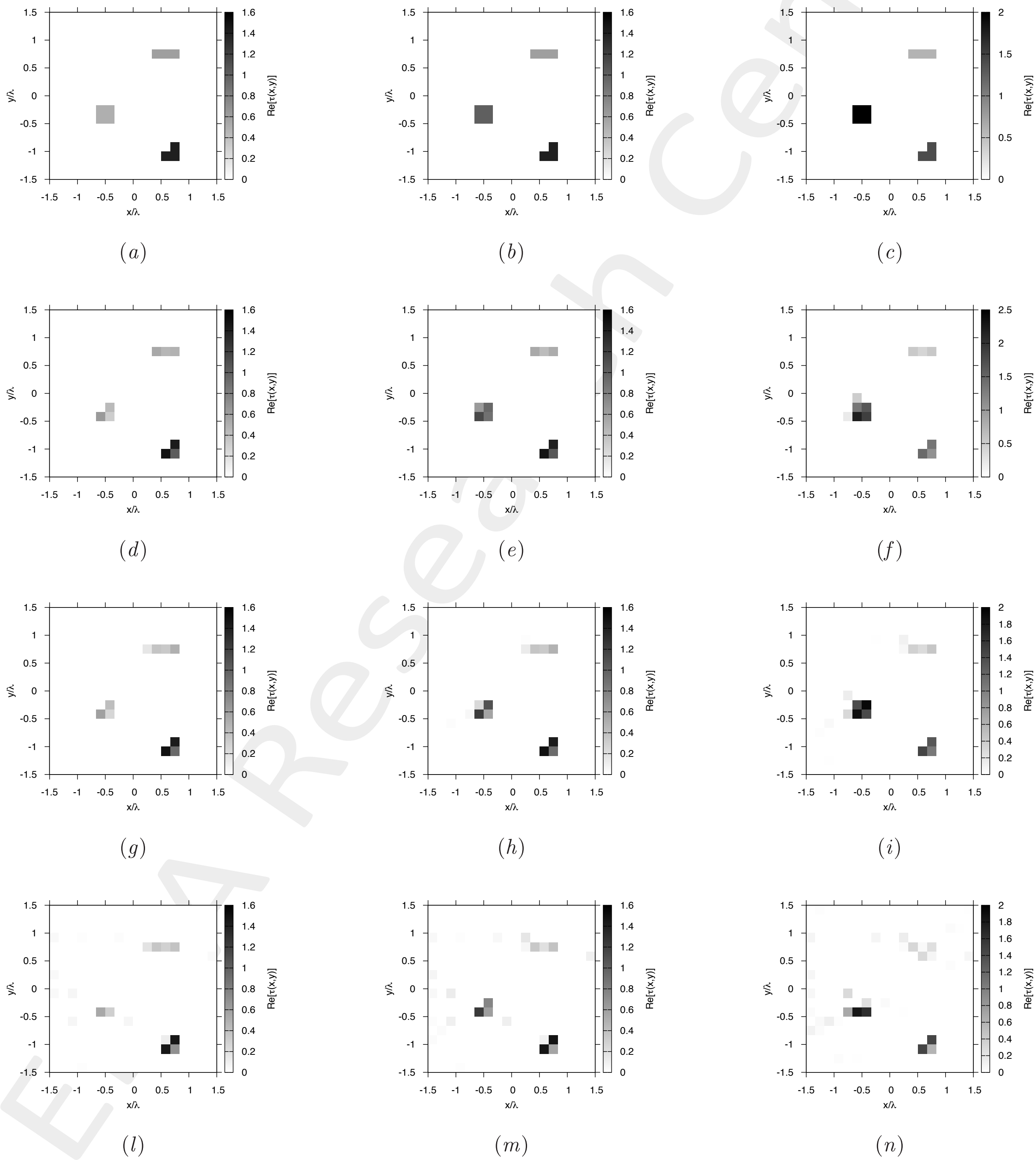

Figure 29. Actual object $(a)(b)(c)$ and MF-MT-BCS reconstructed object with $\varepsilon_r = 1.5$ $(d)(g)(l)$, $\varepsilon_r = 2.0$ $(e)(h)(m)$, and $\varepsilon_r = 3.0$ $(f)(i)(n)$, for $SNR = 20$ [dB] $(d)(e)(f)$, $SNR = 10$ [dB] $(g)(h)(i)$ and $SNR = 5$ [dB] $(l)(m)(n)$.

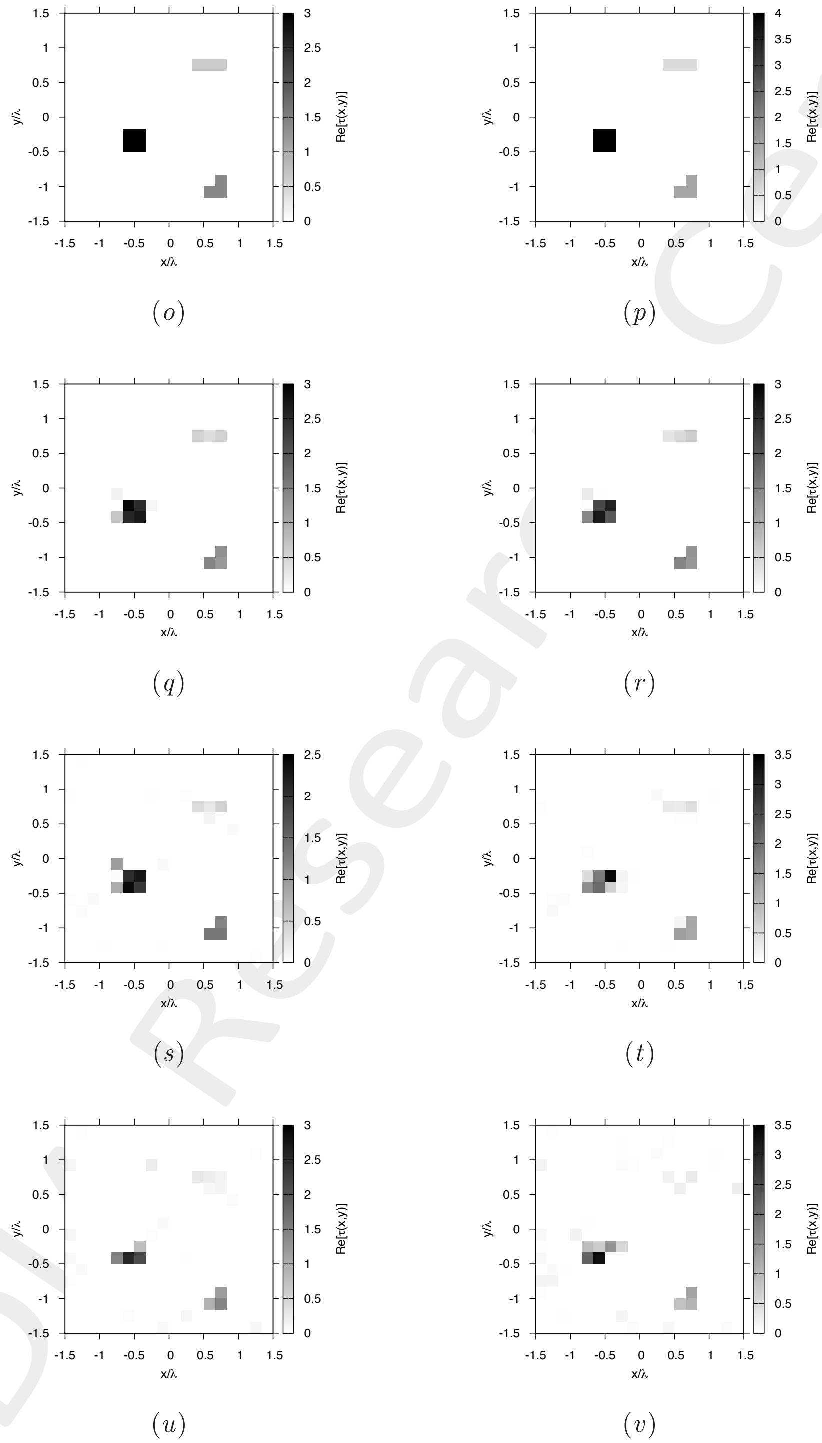

Figure 29. Actual object $(o)(p)$ and MF-MT-BCS reconstructed object with $\varepsilon_r = 4.0$ $(q)(s)(u)$, $\varepsilon_r = 5.0$ $(r)(t)(v)$, for $SNR = 20$ [dB] $(q)(r)$, $SNR = 10$ [dB] $(s)(t)$ and $SNR = 5$ [dB] $(u)(v)$.

Three Non-Homogeneous Objects of Different Shapes - Error Figures vs. ε_r

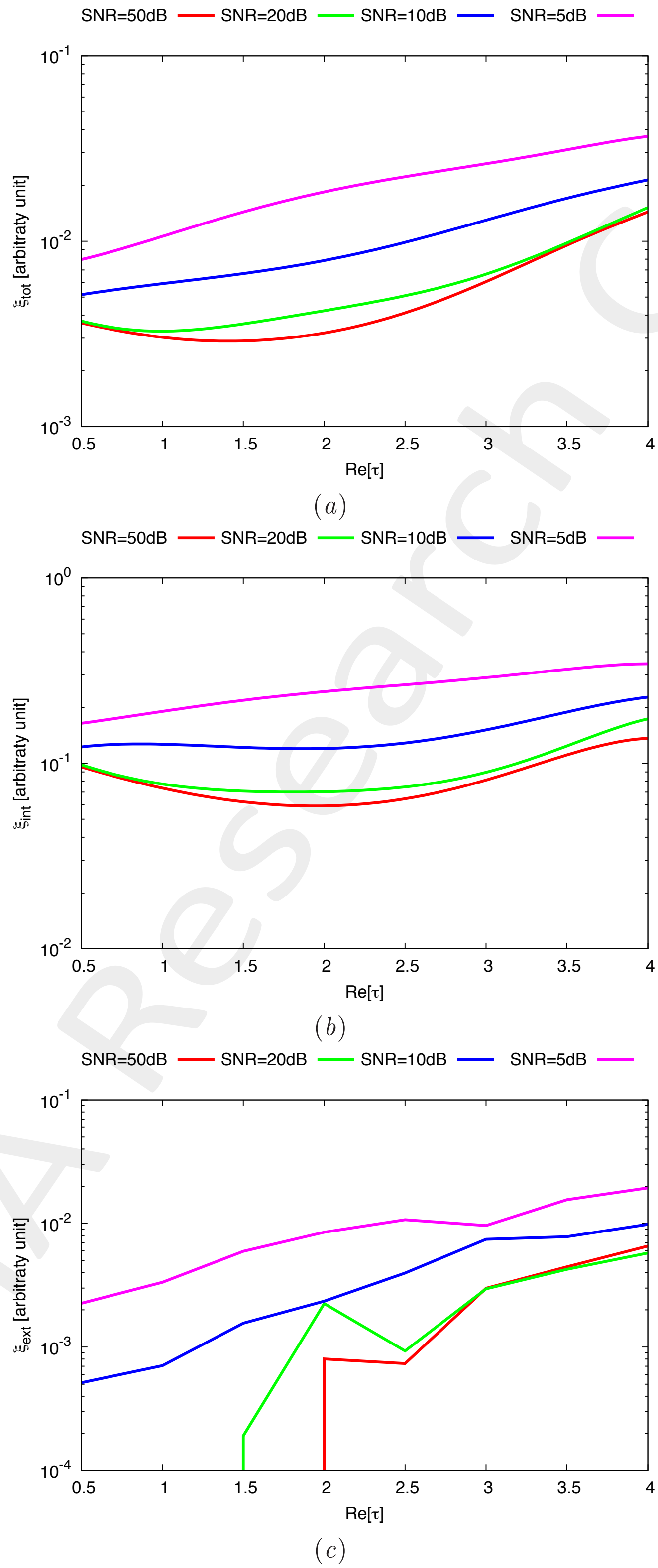

Figure 30. Behaviour of error figures as a function of ε_r, for different SNR values: (a) total error ξ_{tot}, (b) internal error ξ_{int}, (c) external error ξ_{ext}.

Three Non-Homogeneous Objects of Different Shapes - Error Figures vs. SNR

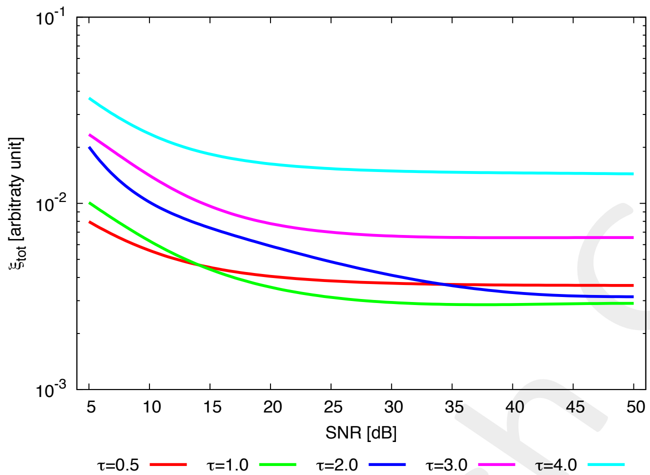

(a)

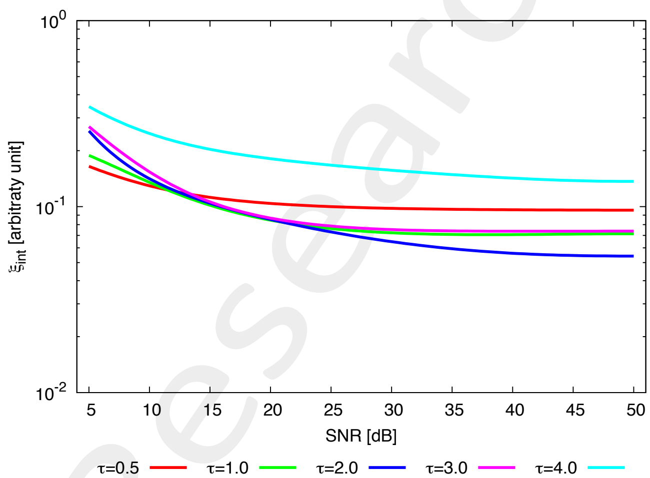

(b)

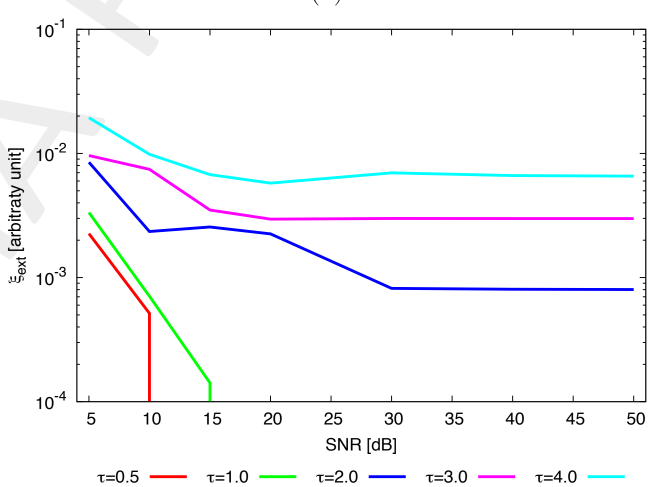

(c)

Figure 31. Behaviour of error figures as a function of SNR, for different ε_r values: (a) total error ξ_{tot}, (b) internal error ξ_{int}, (c) external error ξ_{ext}.

2.2.3 Rectangle of Sides $l_1 = 0.66\lambda$, $l_2 = 0.33\lambda$ and Square of Side $l_3 = 0.33\lambda$

Goal: show the performances of the multi-frequency $MT-BCS$ when dealing with a sparse scatterer

- Number of frequencies F
- Number of Views: V
- Number of Measurements: M
- Number of Cells for the Inversion: N
- Number of Cells for the Direct solver: D
- Side of the investigation domain: L

Test Case Description

Direct solver:

- Square domain divided in $\sqrt{D} \times \sqrt{D}$ cells
- Domain side: $L = 3\lambda$ (at the central frequency)
- $D = 1296$ (discretization for the direct solver: $< \lambda/10$)

Investigation domain:

- Square domain divided in $\sqrt{N} \times \sqrt{N}$ cells
- $L = 3\lambda$
- $2ka = 2 \times \frac{2\pi}{\lambda} \times \frac{L\sqrt{2}}{2} = 6\pi\sqrt{2} = 26.65$
- $\#DOF = \frac{(2ka)^2}{2} = \frac{(2\times\frac{2\pi}{\lambda}\times\frac{L\sqrt{2}}{2})^2}{2} = 4\pi^2\left(\frac{L}{\lambda}\right)^2 = 4\pi^2 \times 9 \approx 355.3$
- N scelto in modo da essere vicino a $\#DOF$: $N = 324$ (18×18)

Measurement domain:

- Measurement points taken on a circle of radius $\rho = 3\lambda$ (at the central frequency)
- $M \approx 2ka \rightarrow M = 27$

Sources:

- $V = 1$ $(\theta = 0°)$
- Amplitude: $A = 1$ (plane waves)
- Number of Frequencies: $F = 11$
- Frequency Range: $I_F = [150\,Mhz : 450MHz]$ - Frequency Step: $S_F = [30\,Mhz]$

Object:

- Rectangle of sides $l_1^{obj_1} = 0.33\lambda$, $l_2^{obj_1} = 0.66\lambda$; Square of sides $l^{obj_2} = 0.33\lambda$
- $\varepsilon_r^{obj_1} = 1.9$, $\varepsilon_r^{obj_2} \in \{1.5, 2.0, 2.5, 3.0, 3.5, 4.0, 4.5, 5.0\}$
- $\sigma = 0$ [S/m]

MT-BCS parameters:

- Gamma prior on noise variance parameters: $\beta_1 = 6.5 \times 10^{-1}$, $\beta_2 = 5.8 \times 10^{-2}$
- Convergenze parameter: $\tau = 1.0 \times 10^{-8}$

Non-Homogeneous Rectangle of Sides $l_1^{obj_1} = 0.66\lambda$, $l_2^{obj_1} = 0.33\lambda$ and Square of Side $l^{obj_2} = 0.33\lambda$ - Reconstruction Profiles

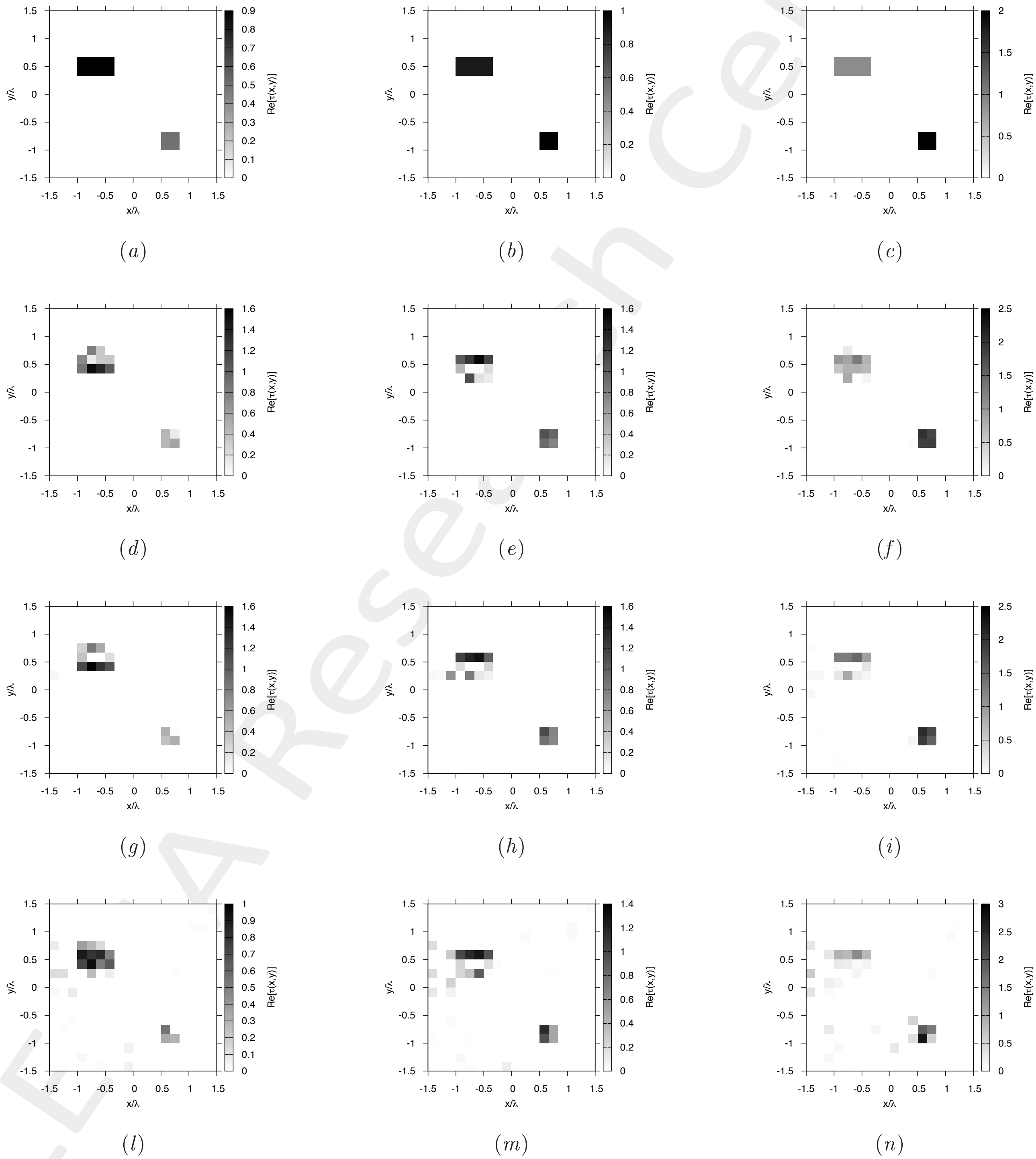

Figure 32. Actual object $(a)(b)(c)$ and MF-MT-BCS reconstructed object with $\varepsilon_r = 1.5$ $(d)(g)(l)$, $\varepsilon_r = 2.0$ $(e)(h)(m)$, and $\varepsilon_r = 3.0$ $(f)(i)(n)$, for $SNR = 20$ [dB] $(d)(e)(f)$, $SNR = 10$ [dB] $(g)(h)(i)$ and $SNR = 5$ [dB] $(l)(m)(n)$.

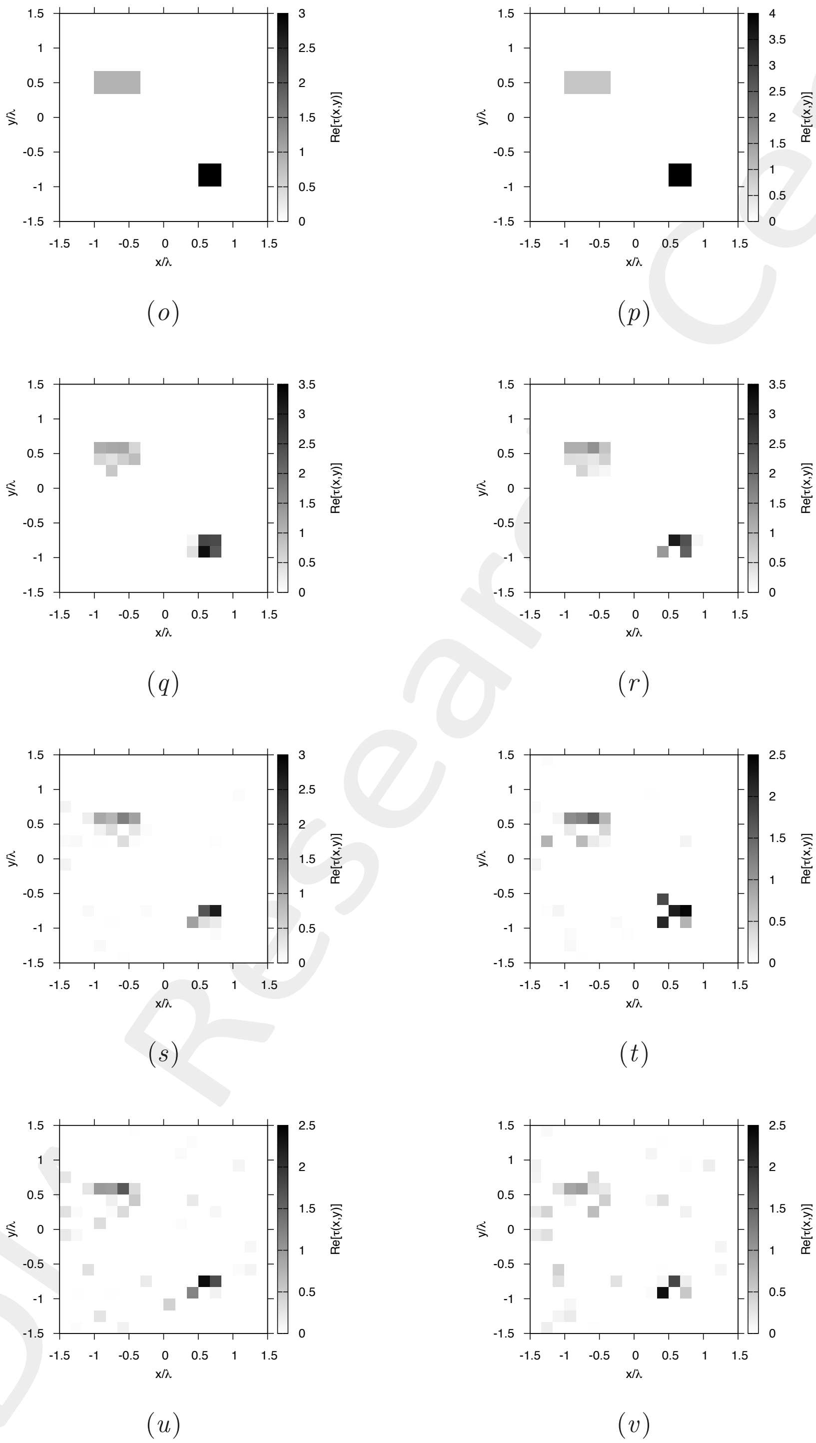

Figure 32. Actual object $(o)(p)$ and MF-MT-BCS reconstructed object with $\varepsilon_r = 4.0$ $(q)(s)(u)$, $\varepsilon_r = 5.0$ $(r)(t)(v)$, for $SNR = 20$ [dB] $(q)(r)$, $SNR = 10$ [dB] $(s)(t)$ and $SNR = 5$ [dB] $(u)(v)$.

Non-Homogeneous Rectangle of Sides $l_1^{obj_1} = 0.66\lambda$, $l_2^{obj_1} = 0.33\lambda$ and Square of Side $l^{obj_2} = 0.33\lambda$ - Error Figures vs. ε_r

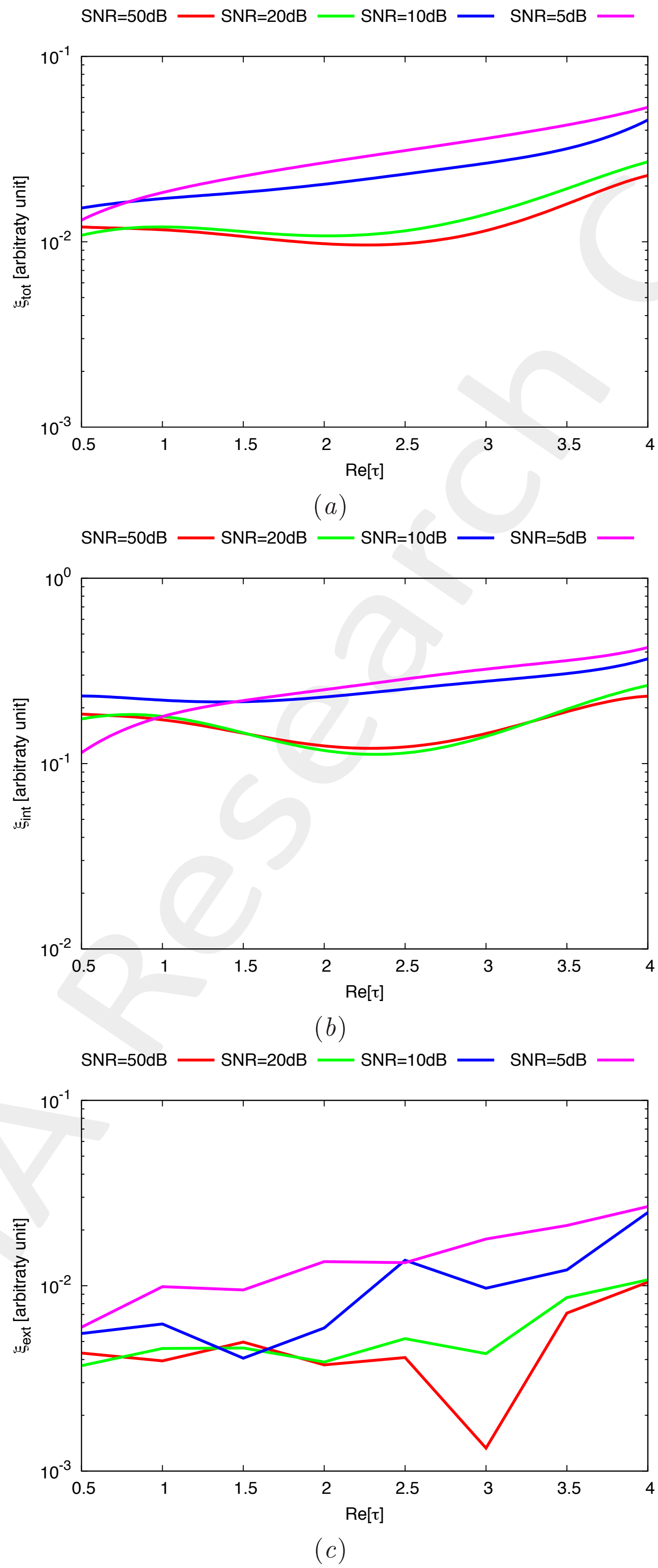

Figure 33. Behaviour of error figures as a function of ε_r, for different SNR values: (a) total error ξ_{tot}, (b) internal error ξ_{int}, (c) external error ξ_{ext}.

Non-Homogeneous Rectangle of Sides $l_1^{obj_1} = 0.66\lambda$, $l_2^{obj_1} = 0.33\lambda$ and Square of Side $l^{obj_2} = 0.33\lambda$ - Error Figures vs. SNR

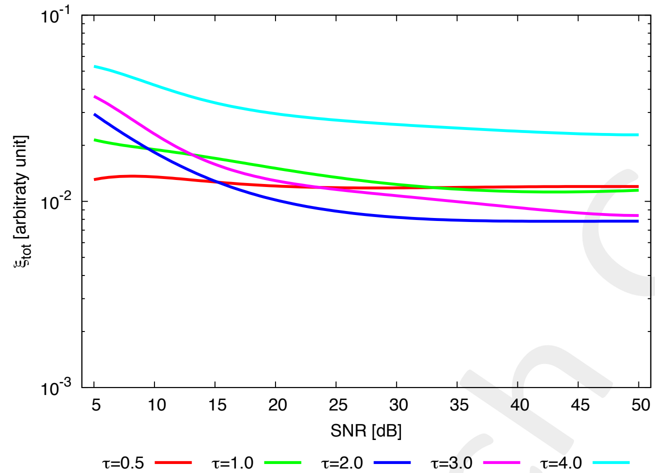

(a)

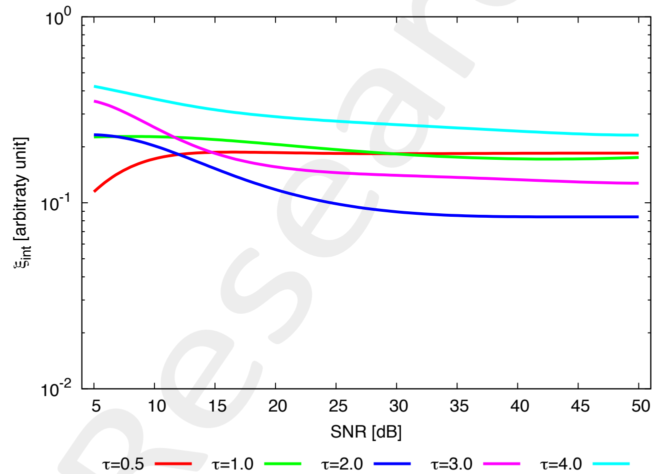

(b)

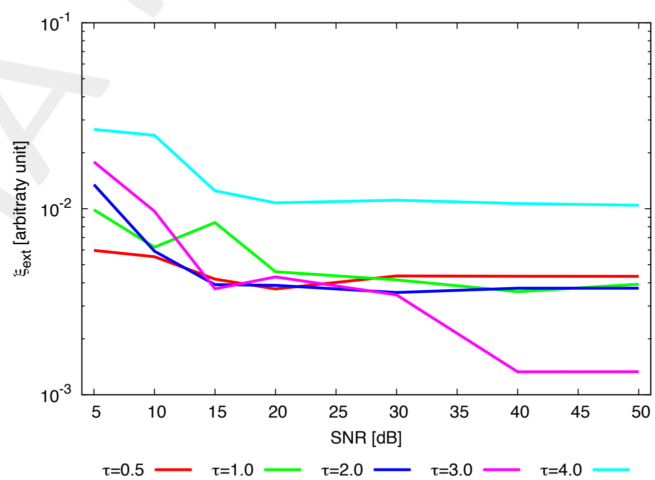

(c)

Figure 34. Behaviour of error figures as a function of SNR, for different ε_r values: (a) total error ξ_{tot}, (b) internal error ξ_{int}, (c) external error ξ_{ext}.

3 Varying the Nr. of Frequencies

3.1 Homogeneous Objects

3.1.1 Three Objects Different Shapes

Goal: show the performances of the multi-frequency $MT - BCS$ when dealing with a sparse scatterer

- Number of frequencies F
- Number of Views: V
- Number of Measurements: M
- Number of Cells for the Inversion: N
- Number of Cells for the Direct solver: D
- Side of the investigation domain: L

Test Case Description

Direct solver:

- Square domain divided in $\sqrt{D} \times \sqrt{D}$ cells
- Domain side: $L = 3\lambda$ (at the central frequency)
- $D = 1296$ (discretization for the direct solver: $< \lambda/10$)

Investigation domain:

- Square domain divided in $\sqrt{N} \times \sqrt{N}$ cells
- $L = 3\lambda$
- $2ka = 2 \times \frac{2\pi}{\lambda} \times \frac{L\sqrt{2}}{2} = 6\pi\sqrt{2} = 26.65$
- $\#DOF = \frac{(2ka)^2}{2} = \frac{(2\times\frac{2\pi}{\lambda}\times\frac{L\sqrt{2}}{2})^2}{2} = 4\pi^2\left(\frac{L}{\lambda}\right)^2 = 4\pi^2 \times 9 \approx 355.3$
- N scelto in modo da essere vicino a $\#DOF$: $N = 324$ (18×18)

Measurement domain:

- Measurement points taken on a circle of radius $\rho = 3\lambda$ (at the central frequency)
- $M \approx 2ka \rightarrow M = 27$

Sources:

- $V = 1$ $(\theta = 0°)$
- Amplitude: $A = 1$ (plane waves)
- Number of Frequencies: $F = \in \{3, 5, 7, 11\}$
- Frequency Range: $I_F = [150\,Mhz : 450MHz]$ - Frequency Step: $S_F = [30\,Mhz]$

Object:

- Strip of sides $l_1^{obj_1} = 0.16\lambda$, $l_2^{obj_1} = 0.50\lambda$; Square cylinder of side $l^{obj_2} = 0.33\lambda$; L-shaped cylinder
- $\varepsilon_r = \in \{1.5, 2.0, 2.5, 3.0, 3.5, 4.0, 4.5, 5.0\}$
- $\sigma = 0$ [S/m]

BCS parameters:

- Gamma prior on noise variance parameters: $\beta_1 = 6.5 \times 10^{-1}$, $\beta_2 = 5.8 \times 10^{-2}$
- Convergenze parameter: $\tau = 1.0 \times 10^{-8}$

Three Homogeneous Objects of Different Shapes - Varying the Nr. of Frequencies - Error Figures vs. ε_r - $SNR = 50$ [dB]

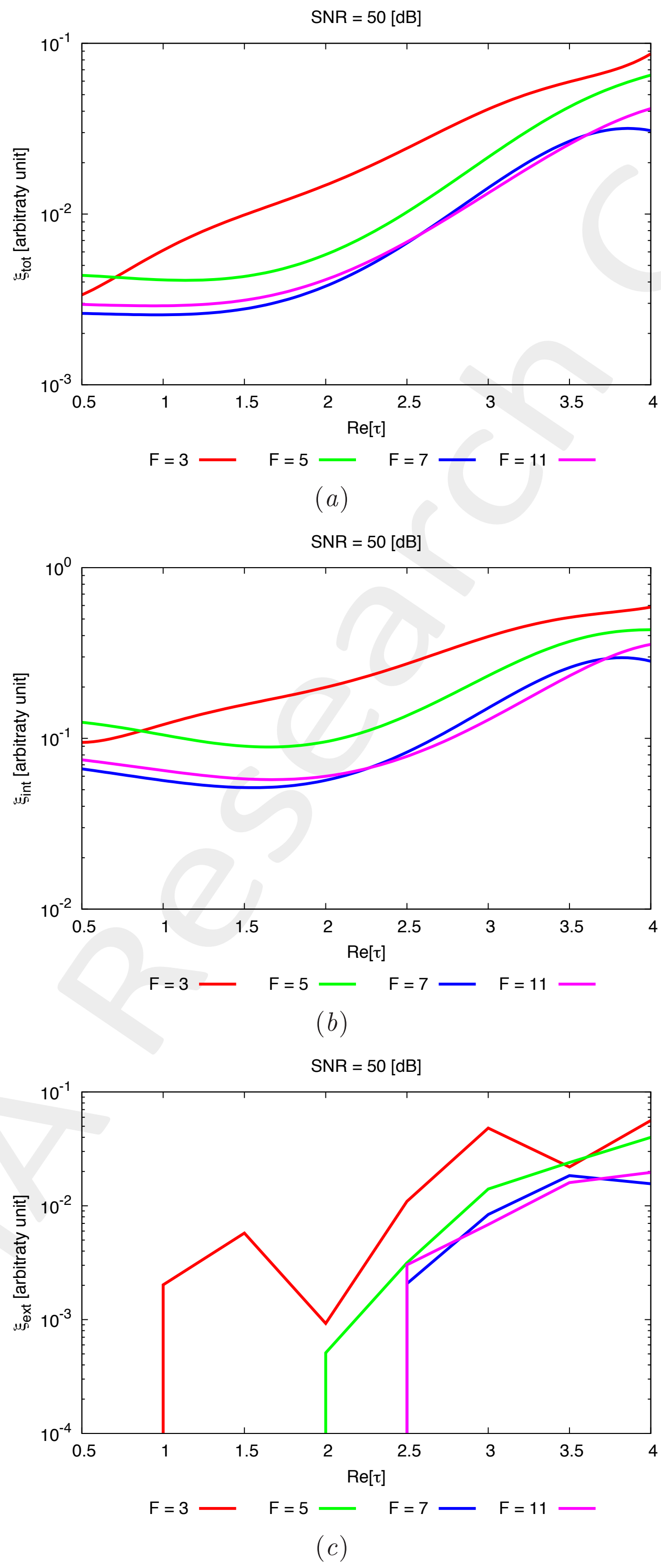

Figure 121. *Varying the Nr. of Frequencies* - Behaviour of error figures as a function of ε_r, for different F values: (a) total error ξ_{tot}, (b) internal error ξ_{int}, (c) external error ξ_{ext}.

Three Homogeneous Objects of Different Shapes - Varying the Nr. of Frequencies - Error Figures vs. ε_r - $SNR = 20$ [dB]

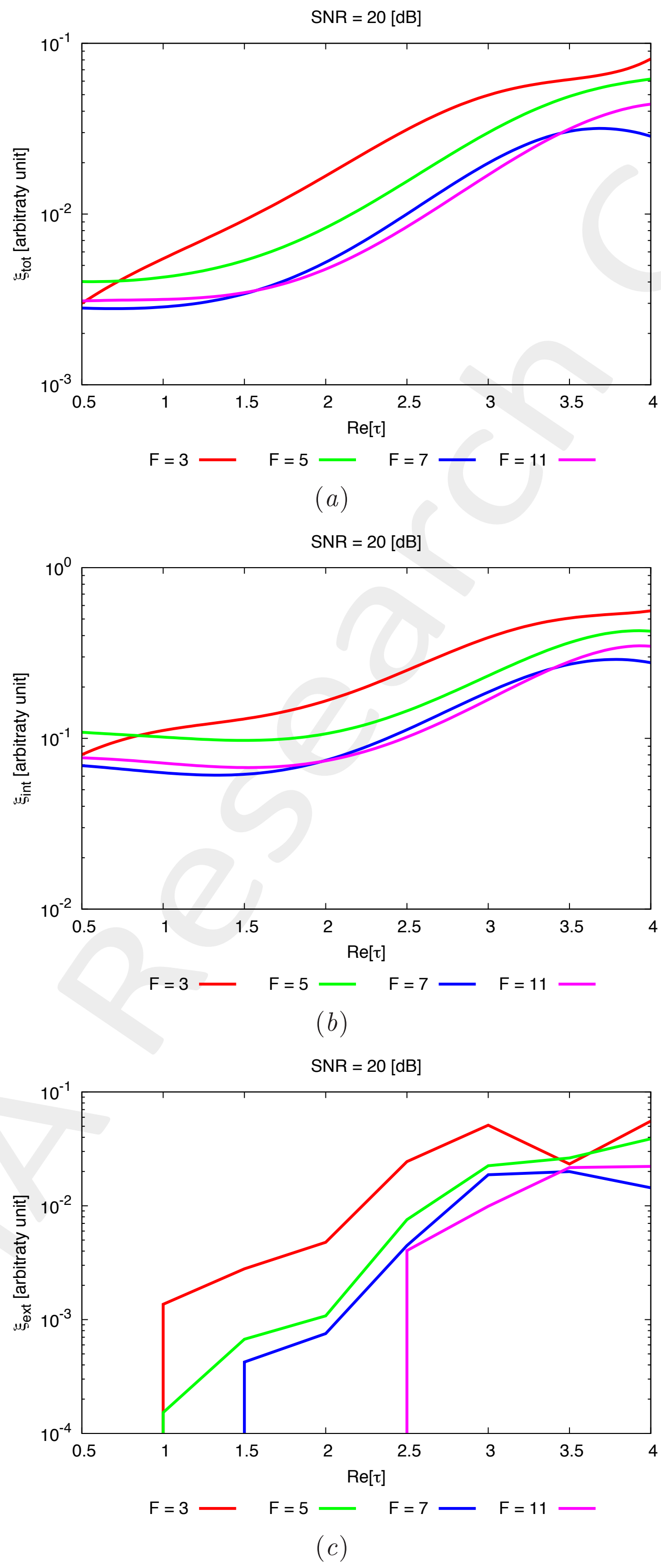

Figure 122. *Varying the Nr. of Frequencies* - Behaviour of error figures as a function of ε_r, for different F values: (a) total error ξ_{tot}, (b) internal error ξ_{int}, (c) external error ξ_{ext}.

Three Homogeneous Objects of Different Shapes - Varying the Nr. of Frequencies - Error Figures vs. ε_r - $SNR = 10$ [dB]

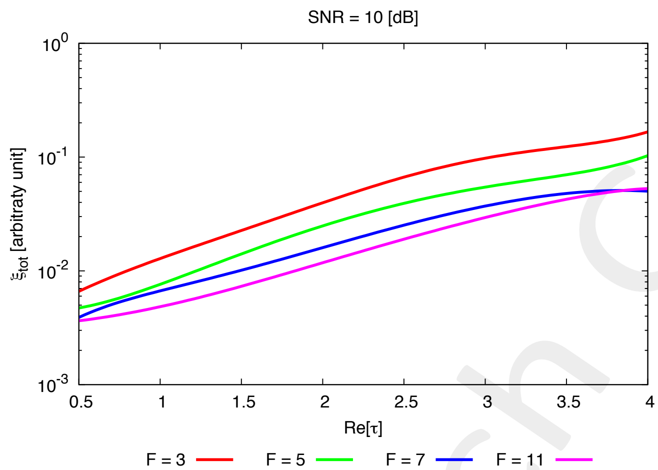

(a)

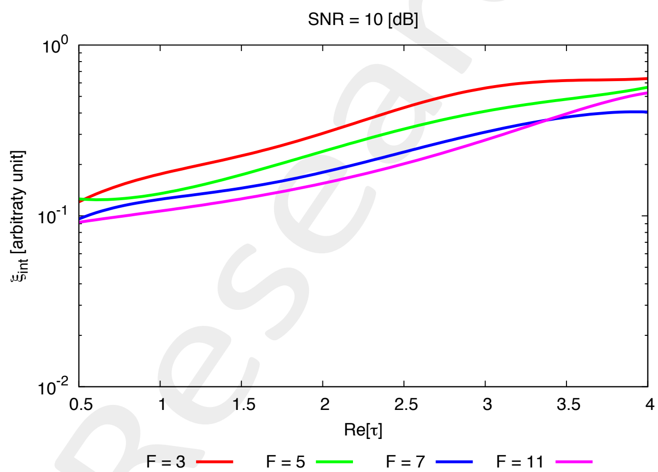

(b)

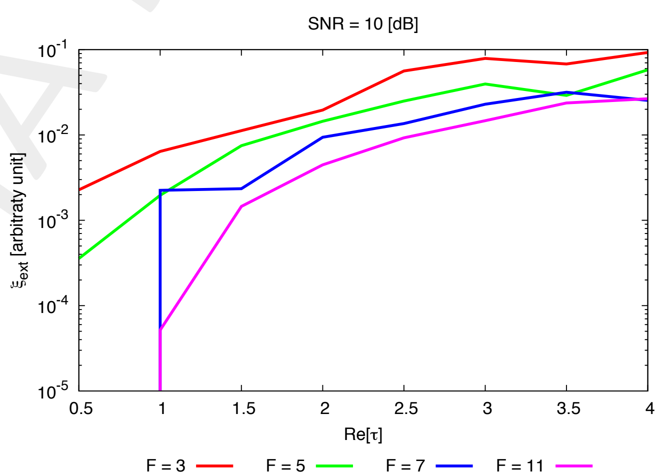

(c)

Figure 123. *Varying the Nr. of Frequencies* - Behaviour of error figures as a function of ε_r, for different F values: (a) total error ξ_{tot}, (b) internal error ξ_{int}, (c) external error ξ_{ext}.

Three Homogeneous Objects of Different Shapes - Varying the Nr. of Frequencies - Error Figures vs. ε_r - $SNR = 5$ [dB]

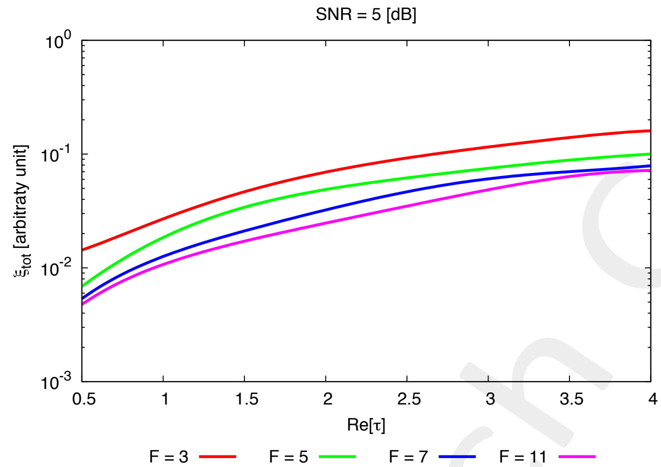

(a)

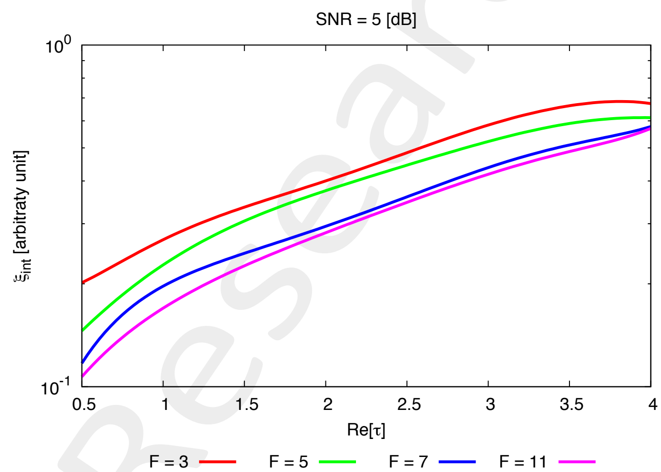

(b)

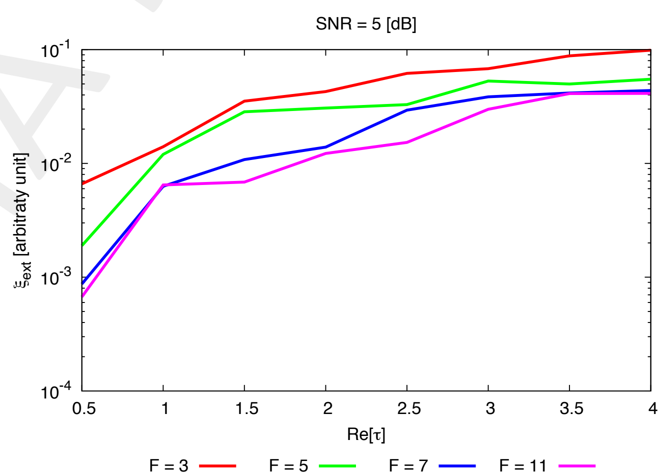

(c)

Figure 124. *Varying the Nr. of Frequencies* - Behaviour of error figures as a function of ε_r, for different F values: (a) total error ξ_{tot}, (b) internal error ξ_{int}, (c) external error ξ_{ext}.

3.2 Non-Homogeneous Objects

3.2.1 Two Strips of Sides $l_1 = 0.16\lambda$, $l_2 = 0.50\lambda$

Goal: show the performances of the multi-frequency $MT - BCS$ when dealing with a sparse scatterer

- Number of frequencies F
- Number of Views: V
- Number of Measurements: M
- Number of Cells for the Inversion: N
- Number of Cells for the Direct solver: D
- Side of the investigation domain: L

Test Case Description

Direct solver:

- Square domain divided in $\sqrt{D} \times \sqrt{D}$ cells
- Domain side: $L = 3\lambda$ (at the central frequency)
- $D = 1296$ (discretization for the direct solver: $< \lambda/10$)

Investigation domain:

- Square domain divided in $\sqrt{N} \times \sqrt{N}$ cells
- $L = 3\lambda$
- $2ka = 2 \times \frac{2\pi}{\lambda} \times \frac{L\sqrt{2}}{2} = 6\pi\sqrt{2} = 26.65$
- $\#DOF = \frac{(2ka)^2}{2} = \frac{(2 \times \frac{2\pi}{\lambda} \times \frac{L\sqrt{2}}{2})^2}{2} = 4\pi^2 \left(\frac{L}{\lambda}\right)^2 = 4\pi^2 \times 9 \approx 355.3$
- N scelto in modo da essere vicino a $\#DOF$: $N = 324$ (18×18)

Measurement domain:

- Measurement points taken on a circle of radius $\rho = 3\lambda$ (at the central frequency)
- $M \approx 2ka \rightarrow M = 27$

Sources:

- $V = 1$ $(\theta = 0°)$
- Amplitude: $A = 1$ (plane waves)
- Number of Frequencies: $F = 11$
- Frequency Range: $I_F = [150\, Mhz\, :\, 450 MHz]$ - Frequency Step: $S_F = [30\, Mhz]$

Object:

- Two strips of sides $l_1 = 0.16\lambda$, $l_2 = 0.50\lambda$
- $\varepsilon_r^{obj_1} \in \{1.5, 2.0, 2.5, 3.0, 3.5, 4.0, 4.5, 5.0\}$, $\varepsilon_r^{obj_2} = 1.6$
- $\sigma = 0$ [S/m]

BCS parameters:

- Gamma prior on noise variance parameter: $\beta_1 = 6.5 \times 10^{-1}$, $\beta_2 = 5.8 \times 10^{-2}$
- Convergenze parameter: $\tau = 1.0 \times 10^{-8}$

Two Non-Homogeneous Strips of Sides $l_1 = 0.16\lambda$, $l_2 = 0.50\lambda$ - Varying the Nr. of Frequencies - Error Figures vs. ε_r - $SNR = 50$ [dB]

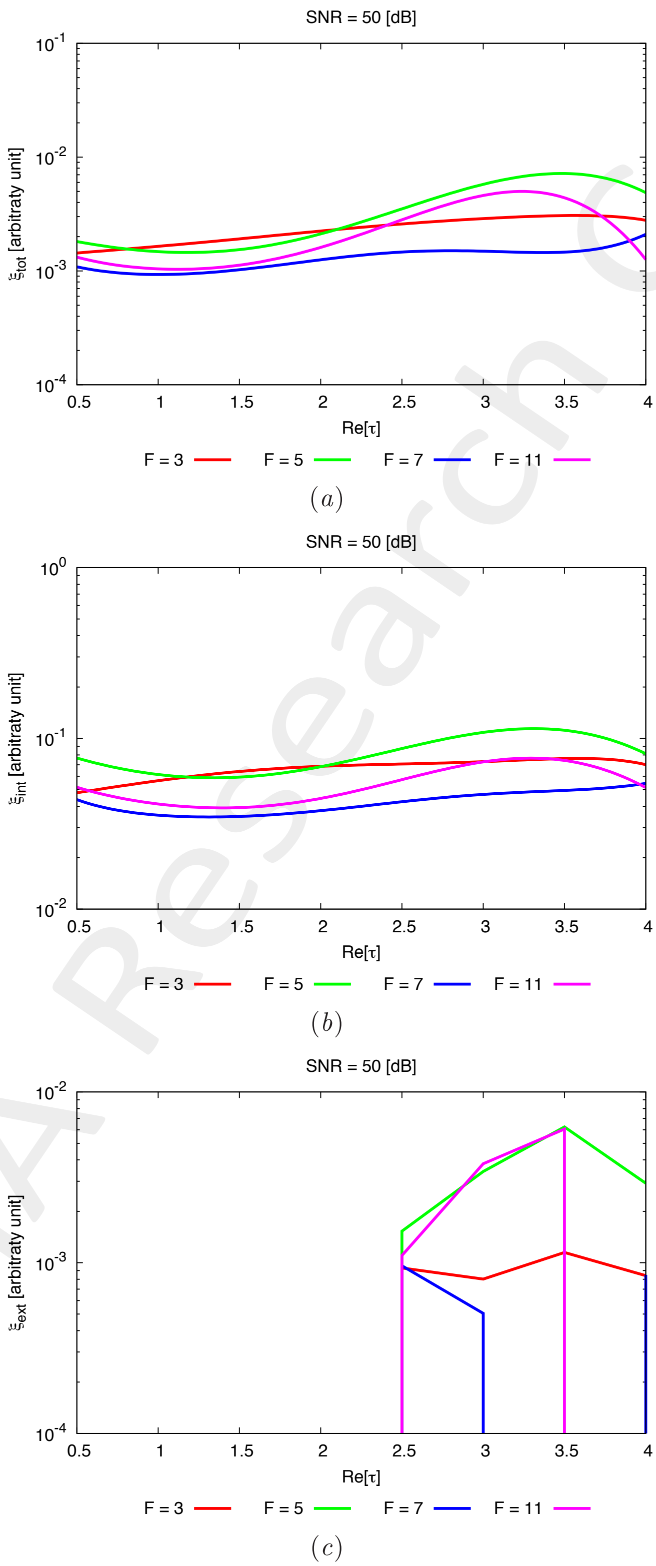

Figure 125. *Varying the Nr. of Frequencies* - Behaviour of error figures as a function of ε_r, for different F values: (a) total error ξ_{tot}, (b) internal error ξ_{int}, (c) external error ξ_{ext}.

Two Non-Homogeneous Strips of Sides $l_1 = 0.16\lambda$, $l_2 = 0.50\lambda$ - Varying the Nr. of Frequencies - Error Figures vs. ε_r - $SNR = 20$ [dB]

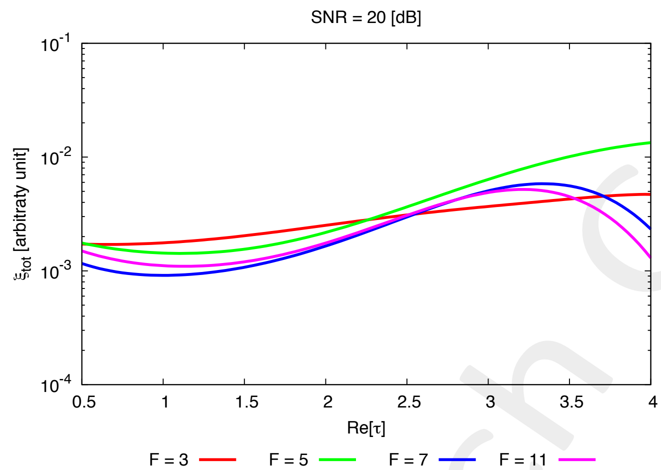

(a)

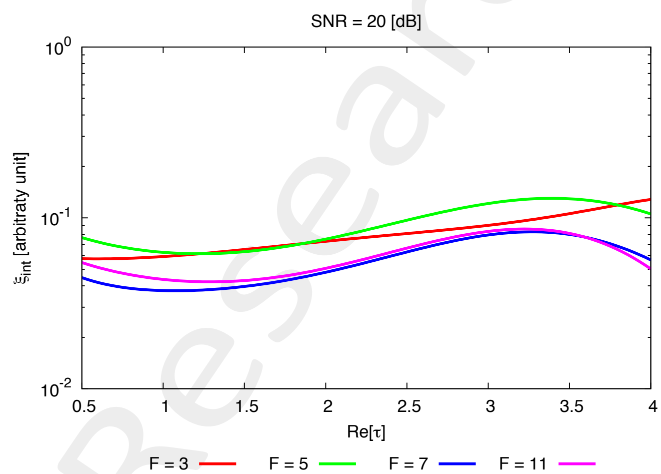

(b)

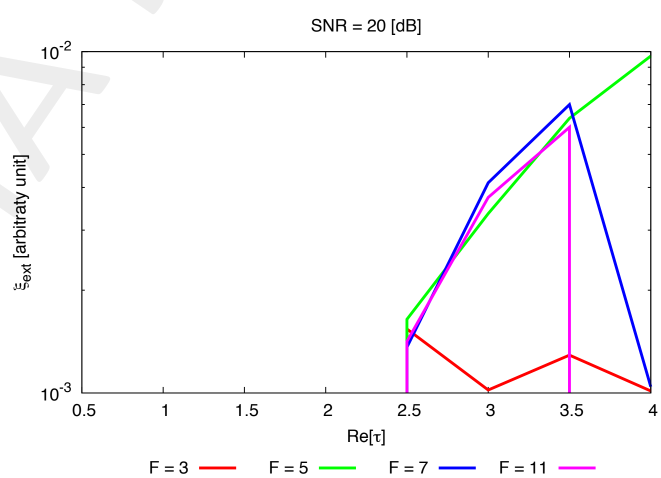

(c)

Figure 126. *Varying the Nr. of Frequencies* - Behaviour of error figures as a function of ε_r, for different F values: (a) total error ξ_{tot}, (b) internal error ξ_{int}, (c) external error ξ_{ext}.

Two Non-Homogeneous Strips of Sides $l_1 = 0.16\lambda$, $l_2 = 0.50\lambda$ - Varying the Nr. of Frequencies - Error Figures vs. ε_r - $SNR = 10$ [dB]

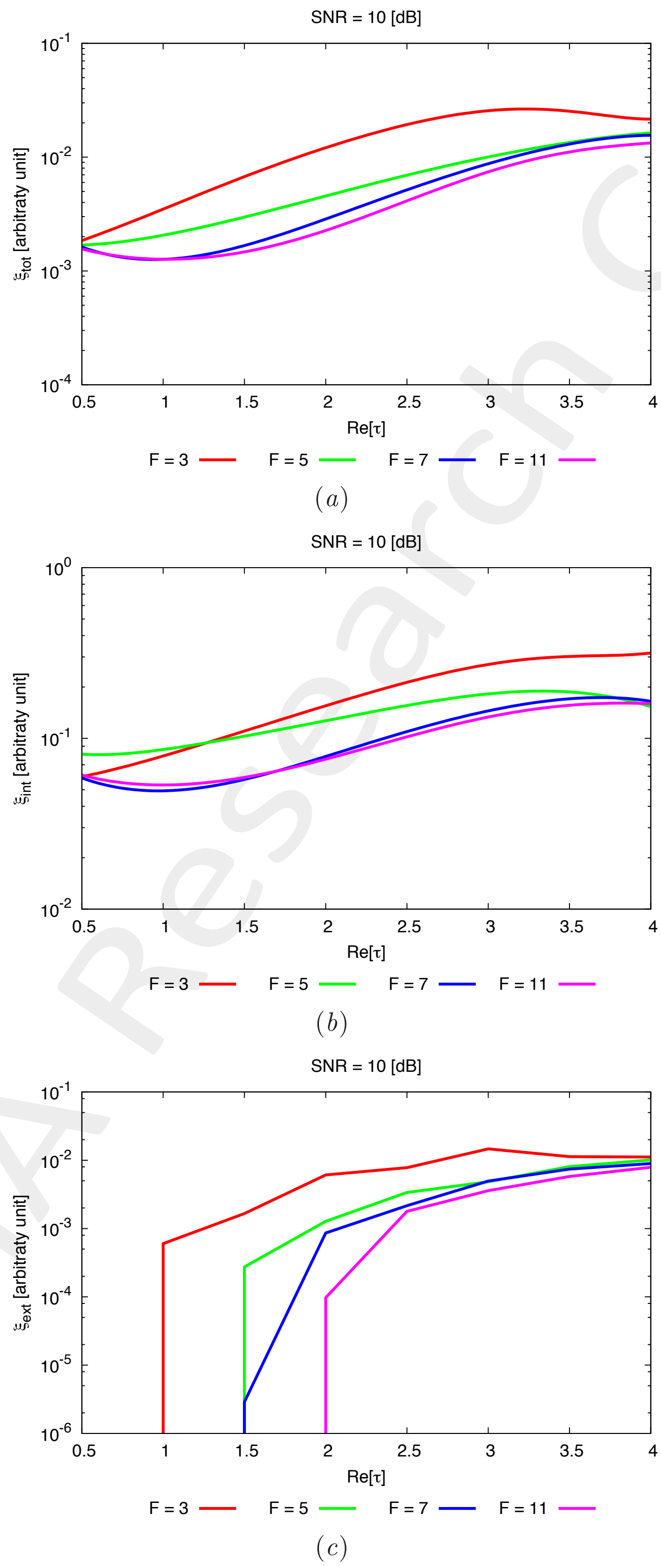

Figure 127. *Varying the Nr. of Frequencies* - Behaviour of error figures as a function of ε_r, for different F values: (a) total error ξ_{tot}, (b) internal error ξ_{int}, (c) external error ξ_{ext}.

Two Non-Homogeneous Strips of Sides $l_1 = 0.16\lambda$, $l_2 = 0.50\lambda$ - Varying the Nr. of Frequencies - Error Figures vs. ε_r - $SNR = 5$ [dB]

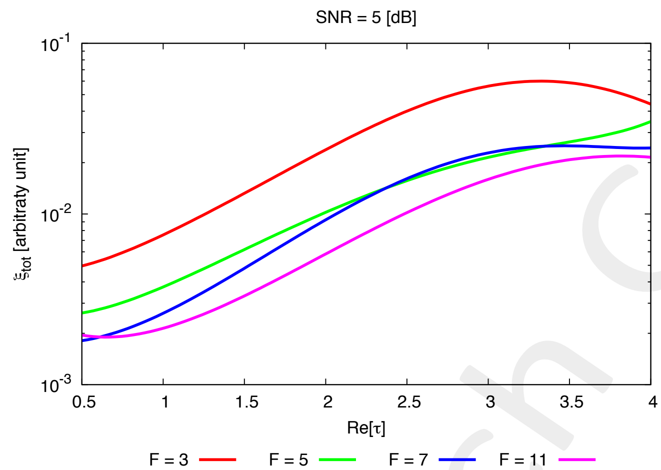

(a)

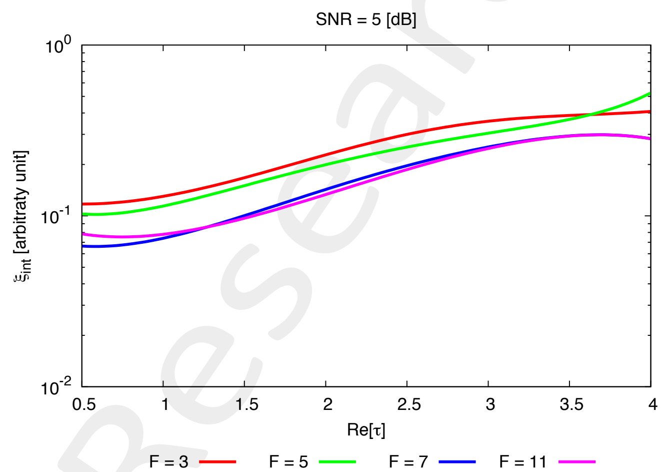

(b)

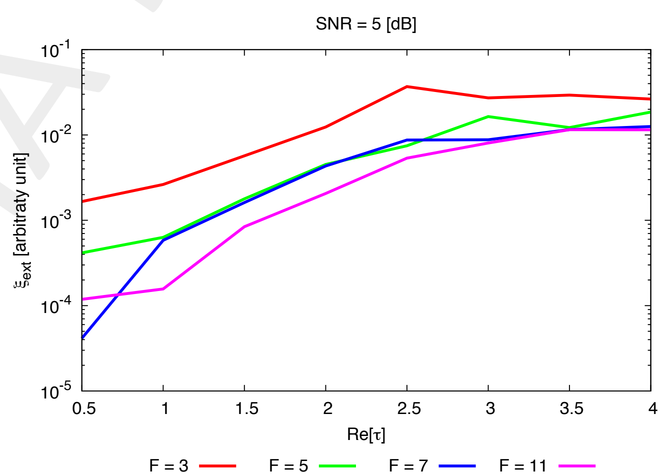

(c)

Figure 128. *Varying the Nr. of Frequencies* - Behaviour of error figures as a function of ε_r, for different F values: (a) total error ξ_{tot}, (b) internal error ξ_{int}, (c) external error ξ_{ext}.

References

[1] G. Oliveri, P. Rocca, and A. Massa, “A Bayesian compressive sampling-based inversion for imaging sparse scatterers,” IEEE Trans. Geosci. Remote Sens., vol. 49, no. 10, pp. 3993-4006, Oct. 2011.

[2] L. Poli, G. Oliveri, P.-P. Ding, T. Moriyama, and A. Massa, "Multifrequency Bayesian compressive sensing methods for microwave imaging," Journal of the Optical Society of the America A, vol. 31, no. 11, pp. 2415-2428, 2014.

[3] G. Oliveri, N. Anselmi, and A. Massa, "Compressive sensing imaging of non-sparse 2D scatterers by a total-variation approach within the Born approximation," IEEE Trans. Antennas Propag., vol. 62, no. 10, pp. 5157-5170, Oct. 2014.

[4] L. Poli, G. Oliveri, and A. Massa, "Imaging sparse metallic cylinders through a Local Shape Function Bayesian Compressive Sensing approach," Journal of Optical Society of America A, vol. 30, no. 6, pp. 1261-1272, 2013.

[5] F. Viani, L. Poli, G. Oliveri, F. Robol, and A. Massa, "Sparse scatterers imaging through approximated multitask compressive sensing strategies," Microwave Opt. Technol. Lett., vol. 55, no. 7, pp. 1553-1558, Jul. 2013.

[6] L. Poli, G. Oliveri, P. Rocca, and A. Massa, "Bayesian compressive sensing approaches for the reconstruction of two-dimensional sparse scatterers under TE illumination," IEEE Trans. Geosci. Remote Sensing, vol. 51, no. 5, pp. 2920-2936, May 2013.

[7] L. Poli, G. Oliveri, and A. Massa, "Microwave imaging within the first-order Born approximation by means of the contrast-field Bayesian compressive sensing," IEEE Trans. Antennas Propag., vol. 60, no. 6, pp. 2865-2879, Jun. 2012.

[8] G. Oliveri, L. Poli, P. Rocca, and A. Massa, "Bayesian compressive optical imaging within the Rytov approximation," Optics Letters, vol. 37, no. 10, pp. 1760-1762, 2012.

[9] L. Poli, G. Oliveri, F. Viani, and A. Massa, "MT-BCS-based microwave imaging approach through minimum-norm current expansion," IEEE Trans. Antennas Propag., vol. 61, no. 9, pp. 4722-4732, Sep. 2013.

[10] G. Oliveri, P.-P. Ding, and L. Poli "3D crack detection in anisotropic layered media through a sparseness-regularized solver," IEEE Antennas Wireless Propag. Lett., in press.

[11] P. Rocca, M. Carlin, L. Manica, and A. Massa, "Microwave imaging within the interval analysis framework," Progress in Electromagnetic Research, vol. 143, pp. 675-708, 2013.

[12] P. Rocca, M. Carlin, G. Oliveri, and A. Massa, "Interval analysis as applied to inverse scattering," IEEE International Symposium on Antennas Propag. (APS/URSI 2013), Chicago, Illinois, USA, Jul. 8-14, 2012.

[13] L. Manica, P. Rocca, M. Salucci, M. Carlin, and A. Massa, "Scattering data inversion through interval analysis under Rytov approximation," 7th European Conference on Antennas Propag. (EuCAP 2013), Gothenburg, Sweden, Apr. 8-12, 2013.

[14] P. Rocca, M. Carlin, and A. Massa, "Imaging weak scatterers by means of an innovative inverse scattering technique based on the interval analysis," 6th European Conference on Antennas Propag. (EuCAP 2012), Prague, Czech Republic, Mar. 26-30, 2012.

[15] G. Oliveri and A. Massa, "Bayesian compressive sampling for pattern synthesis with maximally sparse non-uniform linear arrays," IEEE Trans. Antennas Propag., vol. 59, no. 2, pp. 467-481, Feb. 2011.

[16] G. Oliveri, M. Carlin, and A. Massa, "Complex-weight sparse linear array synthesis by Bayesian Compressive Sampling," IEEE Trans. Antennas Propag., vol. 60, no. 5, pp. 2309-2326, May 2012.

[17] G. Oliveri, P. Rocca, and A. Massa, "Reliable Diagnosis of Large Linear Arrays - A Bayesian Compressive Sensing Approach," IEEE Trans. Antennas Propag., vol. 60, no. 10, pp. 4627-4636, Oct. 2012.

[18] F. Viani, G. Oliveri, and A. Massa, "Compressive sensing pattern matching techniques for synthesizing planar sparse arrays," IEEE Trans. Antennas Propag., vol. 61, no. 9, pp. 4577-4587, Sept. 2013.

[19] G. Oliveri, E. T. Bekele, F. Robol, and A. Massa, "Sparsening conformal arrays through a versatile BCS-based method," IEEE Trans. Antennas Propag., vol. 62, no. 4, pp. 1681-1689, Apr. 2014.

[20] M. Carlin, G. Oliveri, and A. Massa, "Hybrid BCS-deterministic approach for sparse concentric ring isophoric arrays," IEEE Trans. Antennas Propag., vol. 63, no. 1, pp. 378-383, Jan. 2015.